Biocatalysis

International Edition: DOI: 10.1002/anie.201508817
German Edition: DOI: 10.1002/ange.201508817

Myoglobin-Catalyzed Olefination of Aldehydes

*Vikas Tyagi and Rudi Fasan**

Abstract: *The olefination of aldehydes constitutes a most valuable and widely adopted strategy for constructing carbon–carbon double bonds in organic chemistry. While various synthetic methods have been made available for this purpose, no biocatalysts are known to mediate this transformation. Reported herein is that engineered myoglobin variants can catalyze the olefination of aldehydes in the presence of α-diazoesters with high catalytic efficiency (up to 4,900 turnovers) and excellent E diastereoselectivity (92–99.9 % de). This transformation could be applied to the olefination of a variety of substituted benzaldehydes and heteroaromatic aldehydes, also in combination with different alkyl α-diazoacetate reagents. This work provides a first example of biocatalytic aldehyde olefination and extends the spectrum of synthetically valuable chemical transformations accessible using metalloprotein-based catalysts.*

The Wittig reaction[1] represents one of the most valuable and broadly adopted routes for the construction of olefinic bonds during the synthesis of organic molecules.[2] Classically, this method involves the reaction between carbonyl compounds and phosphonium ylides, which are prepared by deprotonation of the corresponding phosphonium salts.[3] Because of the basic conditions required for the latter process, there has been a significant interest toward developing alternative methods to enable the olefination of aldehydes under milder, neutral reaction conditions. In this regard, the transition metal catalyzed transformation of carbonyls in the presence of diazo compounds and tertiary phosphines has provided a particularly attractive strategy because of the ready accessibility of these reagents.[4] Over recent years, a number of organometallic catalysts including Mo,[4a] Re,[4b–d] Rh,[4e] Ir,[4f] Ru,[4g,h] Cu,[4i] and Fe[4j–o] complexes, have proven useful in this transformation, yielding *E*-configured olefins with modest to good catalytic activity (typically, 50-300 turnovers) and moderate to high *E* selectivity (typically, 70–98 % *de*). In contrast to the important progress made in the development of synthetic catalysts for aldehyde olefination, no natural enzyme or artificial biocatalysts[5] has been reported to promote this valuable transformation. An aldehyde olefination biocatayst would thus represent a valuable addition to the toolbox of currently available enzymes for asymmetric synthesis[6].

[*] Dr. V. Tyagi, Prof. Dr. R. Fasan
Department of Chemistry, University of Rochester
120 Trustee Road, Rochester, NY 14627 (USA)
E-mail: fasan@chem.rochester.edu

Supporting information and ORCID(s) from the author(s) for this article are available on the WWW under http://dx.doi.org/10.1002/anie.201508817.

We and others have recently reported the ability of heme-dependent metalloproteins such as cytochrome P450s[7] and myoglobin[8] to engage diazo-containing reagents in carbene-transfer reactions. In particular, we recently discovered that engineered variants of myoglobin can provide particularly efficient catalysts for olefin cyclopropanation,[8a] carbene NH insertion,[8b] and carbene SH insertion reactions[8c] in the presence of α-diazo ester reagents. Our mechanistic studies supported the intermediacy of an electrophilic heme/carbene complex[8a] which reacts with a nucleophilic olefin, amine, or mercaptan to yield the carbene insertion adduct. These studies also showed the possibility to generate a transient sulfonium ylide intermediate upon attack of a thiol substrate to the myoglobin-bound carbenoid species.[8c] Building upon these findings and inspired by pioneering studies conducted by Woo and co-workers with metalloporphyrins,[4j,l] we hypothesized that an analogous process could be exploited in the presence of tertiary phosphine nucleophiles to yield a myoglobin-bound phosphonium ylide. We further envisioned the latter could react with an aldehyde to yield an olefin through a Wittig reaction, with the active site of the protein potentially furnishing an asymmetric environment to influence the stereoselectivity of the reaction. Herein, we report that engineered variants of myoglobin can mediate aldehyde olefination reactions across a range of aldehydes and α-diazoacetates with high catalytic activity and *E* selectivity. This transformation proceeds in buffer and at room temperature, thus providing an extremely mild biocatalytic route for the olefination of aryl and benzylic aldehydes.

Guided by the hypothesis outlined above, we began our studies by testing the ability of wild-type sperm whale myoglobin to promote the conversion of benzaldehyde (**1a**) and ethyl α-diazo acetate (EDA; **2a**) to ethyl cinnamate (**3a**) in the presence of triphenylphosphine (PPh_3). To our delight, we observed formation of the desired product **3a** with good diastereoselectivity (76 % *de* for *E* isomer), albeit with only modest activity [31 turnovers (TON); Table 1, entry 3]. Both reducing ($Na_2S_2O_4$) and oxygen-free conditions were found to be required for the observed Mb-dependent aldehyde olefination activity, indicating that the ferrous form of the hemoprotein is involved in the activation of the diazo compound. Additional experiments showed that hemin can also promote this transformation, but with reduced catalytic efficiency (22 TON) and lower diastereoselectivity (65 % *de*) as compared to Mb (Table 1, entry 1). In addition, the hemin reaction is much less chemoselective, yielding larger amounts of the carbene dimerization byproducts, diethyl fumarate, and diethyl maleate ($TON_{(3a)}/TON_{(4a)}$: 0.4 vs. 2.8 with Mb, Table 1). In an effort to improve the efficiency and selectivity of the Mb-mediated olefination reaction, a variety of trialkyl phosphines [e.g., PEt_3, $P(tBu)_3$, $P(nBu)_3$] as well as heavier congeners of PPh_3 (i.e., $AsPh_3$, $SbPh_3$, and $BiPh_3$) were tested

Table 1: Catalytic activity of hemin and wild-type sperm whale myoglobin (Mb) in the olefination of benzaldehyde with ethyl α-diazoacetate (EDA).[a]

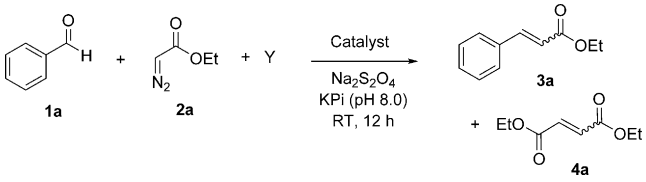

Entry	Catalyst	Y	TON[b] (**3a**)	*de* [%] (*E*)[c]	$TON_{(3a)}$/ $TON_{(4a)}$
1	Hemin	PPh_3	22	64	0.4
2	Hemin[d]	$AsPh_3$	4	91	0.1
3	WT Mb	PPh_3	31	76	2.8
4	WT Mb	$AsPh_3$	27	99.9	0.7
5	WT Mb	$SbPh_3$	5	99.9	0.4
6	WT Mb	$BiPh_3$	0	–	–

[a] Reactions were carried out under anaerobic conditions with 10 mM **1a**, 10 mM **2a**, 20 μM catalyst, 10 mM $Na_2S_2O_4$, and 10 mM **Y** for 12 h at room temperature. [b] TON = mmol olefin/mmol catalyst. Errors in reported values are within ±10%. [c] As determined by chiral-phase gas chromatography. [d] With hemin at 60 μM.

as a substitute for triphenylphosphine (Table 1, entries 4–6). Interestingly, whereas neither $BiPh_3$ nor any of the trialkyl phosphines led to the desired olefin product, the reaction in the presence of $AsPh_3$ exhibited excellent diastereoselectivity, leading to the formation of *trans*-**3a** as the only detectable isomer (> 99.9% *de*).

Encouraged by these results, we extended our investigations to a panel of Mb variants containing one or two mutations at the level of the protein active site. In sperm whale Mb, five amino acid residues (Leu 29, Phe 43, His 64, Val 68, Ile 107) define the cavity located above the distal face of the heme cofactor (see Figure S1 in the Supporting Information).[9] Previously, we found that mutagenesis of these residues had a profound impact on the selectivity and activity of Mb-catalyzed carbene-transfer reactions.[8] Accordingly, Mb active-site variants were tested for their relative activity and selectivity in the olefination of benzaldehyde with EDA in the presence of either PPh_3 or $AsPh_3$.

As summarized in Table 2, the active-site mutations were found to have noticeable effects on the catalytic efficiency (TON), diastereoselectivity, and chemoselectivity of the reaction. Among the Mb variants tested, the double mutant Mb(F43V,V68F), used in combination with $AsPh_3$, emerged as the most promising catalyst for this reaction, exhibiting threefold higher TONs compared to that of the wild-type Mb, excellent diasteroselectivity (> 99.9% *de*), and high chemoselectivity toward aldehyde olefination over carbene dimerization. At a catalyst loading of 0.01 mol%, Mb(F43V,V68F) was determined to support over 1,100 catalytic turnovers for the conversion of **1a** into (*E*)-**3a**, and featured an initial rate of 320 and 40 turnovers per minute over the first minute and first 15 minutes, respectively (see Figure S2 in the Supporting Information). Importantly, nearly absolute *E* selectivity as well as high chemoselectivity ($TON_{(olefin)}$:$TON_{(dimer)}$ > 4) are maintained under these reaction conditions, the latter being

Table 2: Catalytic activity and selectivity of myoglobin variants in benzaldehyde olefination with EDA.[a]

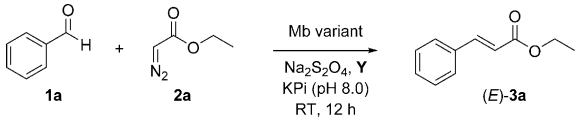

Entry	Catalyst	Y	TON	*de* [%] (*E*)	$TON_{(3a)}$/ $TON_{(4a)}$
1	WT Mb	PPh_3	31	76	2.8
		$AsPh_3$	27	99.9	0.7
2	Mb(L29A)	PPh_3	16	79	0.8
		$AsPh_3$	34	99.9	0.5
3	Mb(F43V)	PPh_3	20	69	1.2
		$AsPh_3$	35	99.9	1.1
4	Mb(F43W)	PPh_3	30	68	6.0
		$AsPh_3$	56	99.9	2.7
5	Mb(H64V)	PPh_3	37	69	1.7
		$AsPh_3$	35	99.9	0.5
6	Mb(V68A)	PPh_3	13	69	0.5
		$AsPh_3$	36	99.9	1.1
7	Mb(V68F)[b]	PPh_3	28	64	0.7
		$AsPh_3$	82	94	1.9
8	Mb(L29A,H64V)	PPh_3	57	70	1.4
		$AsPh_3$	50	80	0.5
9	Mb(H64V,V68A)	PPh_3	7	73	0.8
		$AsPh_3$	16	57	0.2
10	Mb(F43V,V68F)	PPh_3	38	64	2.9
		$AsPh_3$	92	99.9	3.3
11	Mb(F43V,V68F)[c]	$AsPh_3$	1,170	99.9	4.2

[a] Reaction conditions are the same as in Table 1. [b] With 5 μM catalyst (0.05 mol%). [c] With 1 μM catalyst (0.01 mol%).

achieved without the need for slow addition of the diazo compound as typically required for metalloporphyrin catalysts[4h,4j,4n] to minimize carbene dimerization.

Across nearly all Mb variants, the $AsPh_3$-supported reactions consistently furnished higher degrees of diastereoselectivity as compared to those performed in the presence of PPh_3 (Table 2). The only exception was Mb(H64V,V68A), for which a reversal of this trend was observed (70 vs. 57% *de* for reaction with PPh_3 vs. $AsPh_3$). Intriguing is also the differential effect of the active site mutations in the context of this reaction as compared to the carbene-mediated transformations previously investigated by our group.[8] For example, while the double mutation in Mb(H64V,V68A) greatly enhanced the reactivity and selectivity of Mb toward olefin cyclopropanation,[8a] the same mutations led to a reduction in TONs, as well as diastereo- and chemoselectivity for the aldehyde olefination reaction (entry 9 versus 1). These differences highlight the peculiar active-site requirements for favoring high reactivity and selectivity in the context of these related yet mechanistically distinct reactions.

To investigate the scope of Mb(F43V,V68F) as an aldehyde olefination catalyst, the reaction with benzaldehyde **1a** was carried out in the presence of other α-diazo esters, including *tert*-butyl (**2b**), benzyl (**2c**), and cyclohexyl (**2d**) α-diazo acetate as well as ethyl α-diazo-propanoate (**2e**). Notably, despite their variable alkyl chain, all of the α-diazo acetates (**2b–d**) could be readily processed by the biocatalyst to yield the corresponding *trans* β-aryl-α,β-unsaturated ester

Table 3: Catalytic activity and selectivity of Mb(F43V,V68F) variants in benzaldehyde olefination with different α-diazo esters.[a]

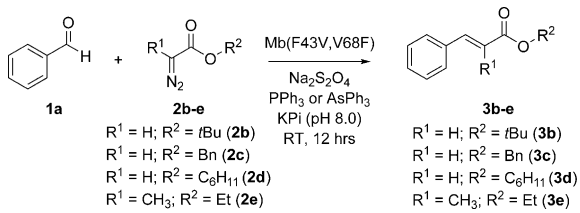

Entry	Product	Y	TON	*de* [%]	Conv. [%][b]
1	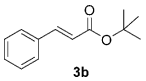	PPh_3	160	79	32
2		$AsPh_3$	40	99.9	8
3[c]	**3b**	$AsPh_3$	175	99.9	1.7
3	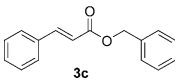	PPh_3	185	83	37
4		$AsPh_3$	155	98	31
5[c]	**3c**	$AsPh_3$	4,920	94	49
5	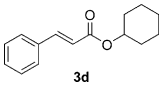	PPh_3	155	79	31
6		$AsPh_3$	205	99.9	41
7[c]	**3d**	$AsPh_3$	4,230	99.9	42

[a] Reaction conditions as described in Table 1 using 20 μM catalyst (0.2 mol%). [b] GC conversion. [c] Using 1 μM catalyst (0.01 mol%).

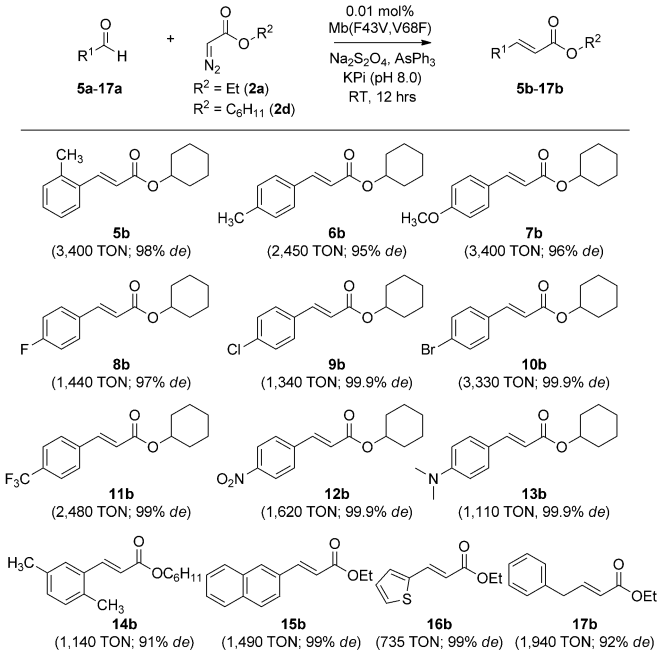

Scheme 1. Substrate scope for Mb(H64V,V68A)-catalyzed aldehyde olefination. Reaction conditions: 10 mM aryl aldehyde, 1 μM Mb(F43V,V68F), 10 mM cyclohexyl α-diazo-acetate (**2d**), 10 mM $AsPh_3$, 10 mM $Na_2S_2O_4$.

products, **3b–d**, with good (79–83% *de*) to excellent (98–99.9% *de*) selectivity in the presence of PPh_3 and $AsPh_3$, respectively (Table 3). In combination with **2c**, Mb(F43V,V68F) gave the highest TON value (4,920) and conversion ratio (49%), whereas the use of the Mb(F43V,V68F)/**2d**/$AsPh_3$ system provided an optimal combination of high catalytic activity (4,230 TON) with excellent stereocontrol (99.9% *de*). As such, the latter system was maintained for further studies on the scope of this hemoprotein across different aldehydes (see below). Under these optimized reaction conditions, the TONs supported by Mb(F43V,V68F) in water and at room temperature are one to two orders of magnitudes higher than those previously reported for similar transformations catalyzed by organometallic complexes in organic solvent and at elevated temperature (50–300 TON[4a–k,m,n]). The only exception is the [Fe(TPP)Cl]-catalyzed olefination of benzaldehyde with EDA and PPh_3 in toluene at 80°C reported by Zhang and coworkers, for which even higher TONs (8,900), but also lower diastereoselectivity (84% *de*) were measured.[4h] In contrast to **2b–d**, no olefination product was observed in the presence of **2e**, thus indicating that α-substitutions on the carbene moiety are not tolerated by the Mb catalyst in the context of this reaction.

Next, the scope of Mb(F43V,V68F)-catalyzed olefination across different aldehyde substrates was investigated. As summarized in Scheme 1, a variety of monosubstituted benzyaldehyde derivatives (**5a–13a**) could be readily converted into the corresponding cyclohexyl *trans*-cinnamate esters **5b–13b** with very good to excellent diastereoselectivities (99–99.9% *de*), with the Mb catalyst supporting from 1,110 (**13b**) to 3,400 turnovers (**5b** and **7b**). Insights into the impact of electronic factors on the efficiency of the reaction could be gained from side-by-side comparison of the TONs for benzaldehyde derivatives carrying substituents of similar size but with different electronic properties. In particular, electron-deficient benzaldehydes were found to be consistently less reactive than their isosteric, electron-richer counterparts, as indicated by the lower TONs measured for **8b** versus **3d**, for **11b** versus **6b**, and **9b** versus **7b**. This trend contrasts with the higher reactivity of electron-poor aldehydes in transition metal catalyzed olefination reactions in organic solvents[4h,j] and it can be rationalized on the basis of the higher level of hydration expected for benzaldehydes carrying electronwithdrawing groups in water.[10] A higher degree of hydration is expected to reduce the effective concentration of aldehyde susceptible to nucleophilic attack by the phoshonium ylide (see below), thus reducing the overall efficiency of the reaction.

The successful conversion of **14a** into **14b** showed that disubstituted benzyaldehydes could be also processed by the Mb(F43V,V68F) catalyst, albeit with lower efficiency (1,140 versus 3,400 TON) and selectivity (91% versus 98% *de*) compared to the monosubstituted counterpart **5b**. Substrates such as 2-naphthaldehyde (**15a**) and thiophene-2-carbaldehyde (**16a**) could also be converted into the corresponding *trans* olefin products **15b** and **16b**, with excellent selectivity (99% *de*), thus further supporting the broad substrate scope of Mb(F43V,V68F) across structurally different aryl aldehydes. Finally, the successful olefination of phenylacetaldehyde (**17a**) to give **17b** (1,940 TON; 92% *de*) demonstrated the reactivity of the catalyst also toward benzylic aldehydes.

A proposed mechanism for the Mb-catalyzed aldehyde olefination reaction is presented in Scheme 2. Starting from the catalytically active ferrous form of the hemoprotein, the

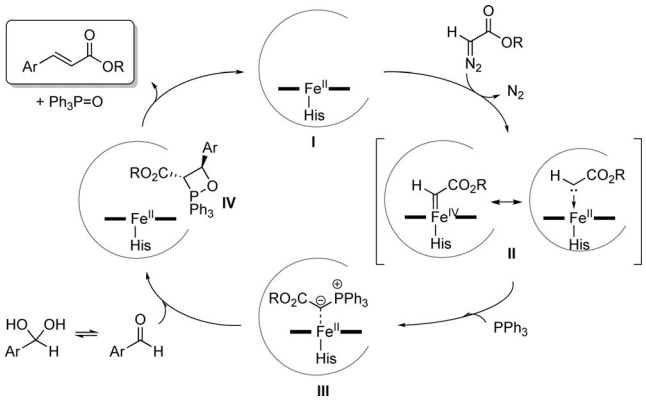

Scheme 2. Proposed mechanism and catalytic steps for the myoglobin-catalyzed olefination of aryl aldehydes.

first step is envisioned to involve the formation of a heme-bound carbenoid intermediate (**II**) upon reaction with the diazo reagent. This intermediate can be formally described as an iron(IV)-carbene complex or as a $Fe^{II}\leftarrow\{:CHCO_2R\}$ complex, the latter being predicted to be a more stable resonance form at least in the context of synthetic iron-porphyrin systems.[11] Regardless of its exact nature, our previous studies showed that this species has electrophilic character[8a] and can react with thiol nucleophiles to generate a transient sulfonium ylide.[8c] Accordingly, attack of the nucleophilic PPh_3 (or $AsPh_3$) to the heme/carbene intermediate is envisioned to ensue, thus giving rise to a phosphonium ylide (**III**). The latter would then react with the aryl aldehyde to generate an oxaphosphetane intermediate[12] (**IV**), whose rearrangement yields the olefin product and phosphine oxide as the byproduct.

In view of the mechanistic model of Scheme 2, a number of considerations can be made in regard of the results described earlier. The first one concerns the role of the biocatalyst on influencing the stereoselectivity of the reaction. Importantly, the Mb reaction with EDA and PPh_3 in the absence of aldehyde was found to accumulate the phosphorane intermediate ($Ph_3P=CHCO_2Et$) in solution, thus supporting the occurrence of the steps **I**→**II**→**III** proposed in Scheme 2. Insightfully, a reaction of premade phosphorane with benzaldehyde yielded (*E*)-**3a** in 80% *de* both in the presence and in the absence of the Mb catalyst. Such diastereoselectivity differs from that observed in the olefination reactions with nearly all of the Mb variants starting from benzaldehyde and EDA (64–76% *de*; Table 2). This result together with the higher diastereoselectivity obtained with Mb versus hemin (Table 1), and the effect of active site mutations on the *E:Z* ratio of the olefin product (Table 2) support the involvement of the protein environment in affecting the stereochemical outcome of the reaction. Since the stereoselectivity of the Wittig reaction is largely dictated by the relative orientation of the ylide and aldehyde during formation of the oxaphosphetane intermediate,[2b,c,12b,15] the asymmetric induction imposed by the hemoprotein scaffold most likely occurs during the conversion of **III** into **IV** (Scheme 2). Possibly, this effect is mediated by coordination of the ylide to the heme iron and/or by interaction of the ylide with the distal cavity of the protein. While Mb has naturally evolved to bind small ligands (i.e. O_2), the steric feasibility of the putative intermediate **III** is suggested by our previous finding that the distal heme pocket in Mb can accommodate rather bulky ligands and substrates.[8,13] This process can be further facilitated by the ability of the distal histidine, His 64 (see Figure S2), to swing open upon ligand binding,[14] thereby creating a larger cavity above the heme.

Another interesting point concerns the structure–reactivity data obtained with the different diazo compounds (Table 3). These studies showed that while relatively large and bulky groups within the ester group of the carbenoid moiety are well tolerated by the Mb(F43V,V68F) catalyst, α-substitutions are not. Since we previously established that ethyl α-diazo propanoate (**2e**) is a viable carbene donor in Mb-catalyzed olefin cyclopropanation,[8a] it can be derived that α-substitutions negatively affect catalytic steps downstream of the formation of the heme/carbene complex during aldehyde olefination. Reasonably, the increased steric hindrance provided by the α-methyl group may disfavor attack of the PPh_3 to the heme/carbene (**II**→**III**; Scheme 2), thus preventing formation of the key phosphonium ylide intermediate.

In spite of the high TON supported by Mb(F43V,V68F), the aldehyde-to-olefin conversion in this reaction was surprisingly found to not exceed 50%. Increasing the α-diazo ester:aldehyde ratio did not improve the yield and resulted in a larger amount of the carbene dimerization product. Through control experiments, catalyst inhibition by action of the aldehyde, phosphine, or olefin product could be ruled out as a possible cause for this phenomenon. A reduction in TON was observed, however, upon addition of increasing amounts of phosphine oxide to the Mb(F43V,V68F)-catalyzed reaction (see Figure S3 in the Supporting Information). Overcoming the inhibitory effect exerted by the phosphine/arsine oxide could thus provide a way to further enhance the efficiency of this Mb-mediated transformation in the future.

In summary, our results show that engineered myoglobins can provide efficient and selective biocatalysts for the olefination of aldehydes under mild and neutral reaction conditions. To our knowledge, this report represents the first example of a biocatalytic strategy for aldehyde olefination. Using the most promising Mb-based catalyst identified in this work, Mb(F43V,V68F), a variety of aryl aldehydes and alkyl α-diazo acetates could be converted into the corresponding olefin products with high catalytic efficiency (1,100–4,900 TON) and very good to excellent *E* selectivity (94–99.9% *de*). The Mb-catalyzed aldehyde olefination reported here contributes to expand the growing number of synthetically valuable transformations accessible through catalysis with engineered and artificial metalloproteins.[5,7–8,13,16]

Acknowledgements

This work was supported by the U.S. National Institute of Health grant GM098628. MS instrumentation was supported by the U.S. NSF grant CHE-0946653.

Keywords: biocatalysis · carbenes · diazo compounds · protein engineering · Wittig reactions

How to cite: *Angew. Chem. Int. Ed.* **2016**, *55*, 2512–2516
Angew. Chem. **2016**, *128*, 2558–2562

[1] G. Wittig, G. Geissler, *Liebigs Ann. Chem.* **1953**, *580*, 44–57.
[2] a) B. E. Maryanoff, A. B. Reitz, *Chem. Rev.* **1989**, *89*, 863–927; b) O. I. Kolodiazhnyi, *Phosphorus Ylides: Chemistry and Applications in Organic Chemistry*, Wiley-VCH, Weinheim, **1999**; c) A. D. Abell, M. K. Edmonds, *Modern Carbonyl Olefination*, Wiley-VCH, Weinheim, **2004**; d) K. C. Nicolaou, M. W. Harter, J. L. Gunzner, A. Nadin, *Liebigs Ann/Recl.* **1997**, 1283–1301; e) H. J. Cristau, *Chem. Rev.* **1994**, *94*, 1299–1313.
[3] X. M. Zhang, F. G. Bordwell, *J. Am. Chem. Soc.* **1994**, *116*, 968–972.
[4] a) X. Y. Lu, H. Fang, Z. J. Ni, *J. Organomet. Chem.* **1989**, *373*, 77–84; b) W. A. Herrmann, M. Wang, *Angew. Chem. Int. Ed. Engl.* **1991**, *30*, 1641–1643; *Angew. Chem.* **1991**, *103*, 1709–1711; c) B. E. Ledford, E. M. Carreira, *Tetrahedron Lett.* **1997**, *38*, 8125–8128; d) A. M. Santos, C. C. Romao, F. E. Kuhn, *J. Am. Chem. Soc.* **2003**, *125*, 2414–2415; e) H. Lebel, V. Paquet, *J. Am. Chem. Soc.* **2004**, *126*, 320–328; f) H. Lebel, C. Ladjel, *Organometallics* **2008**, *27*, 2676–2678; g) E. Graban, F. R. Lemke, *Organometallics* **2002**, *21*, 3823–3826; h) Y. Chen, L. Huang, M. A. Ranade, X. P. Zhang, *J. Org. Chem.* **2003**, *68*, 3714–3717; i) H. Lebel, M. Davi, *Adv. Synth. Catal.* **2008**, *350*, 2352–2358; j) G. A. Mirafzal, G. L. Cheng, L. K. Woo, *J. Am. Chem. Soc.* **2002**, *124*, 176–177; k) Y. Chen, L. Y. Huang, X. P. Zhang, *Org. Lett.* **2003**, *5*, 2493–2496; l) G. L. Cheng, G. A. Mirafzal, L. K. Woo, *Organometallics* **2003**, *22*, 1468–1474; m) V. K. Aggarwal, J. R. Fulton, C. G. Sheldon, J. de Vicente, *J. Am. Chem. Soc.* **2003**, *125*, 6034–6035; n) P. Cao, C. Y. Li, Y. B. Kang, Z. W. Xie, X. L. Sun, Y. Tang, *J. Org. Chem.* **2007**, *72*, 6628–6630; o) C. Y. Li, X. B. Wang, X. L. Sun, Y. Tang, J. C. Zheng, Z. H. Xu, Y. G. Zhou, L. X. Dai, *J. Am. Chem. Soc.* **2007**, *129*, 1494–1495.
[5] a) T. Heinisch, T. R. Ward, *Eur. J. Inorg. Chem.* **2015**, 3406–3418; b) F. T. Yu, V. M. Cangelosi, M. L. Zastrow, M. Tegoni, J. S. Plegaria, A. G. Tebo, C. S. Mocny, L. Ruckthong, H. Qayyum, V. L. Pecoraro, *Chem. Rev.* **2014**, *114*, 3495–3578; c) J. C. Lewis, *ACS Catal.* **2013**, *3*, 2954–2975; d) F. Rosati, G. Roelfes, *ChemCatChem* **2010**, *2*, 916–927.
[6] a) U. T. Bornscheuer, G. W. Huisman, R. J. Kazlauskas, S. Lutz, J. C. Moore, K. Robins, *Nature* **2012**, *485*, 185–194; b) M. T. Reetz, *J. Am. Chem. Soc.* **2013**, *135*, 12480–12496; c) R. Fasan, *ACS Catal.* **2012**, *2*, 647–666; d) N. J. Turner, *Nat. Chem. Biol.* **2009**, *5*, 567–573.
[7] a) P. S. Coelho, E. M. Brustad, A. Kannan, F. H. Arnold, *Science* **2013**, *339*, 307–310; b) P. S. Coelho, Z. J. Wang, M. E. Ener, S. A. Baril, A. Kannan, F. H. Arnold, E. M. Brustad, *Nat. Chem. Biol.* **2013**, *9*, 485–487; c) Z. J. Wang, N. E. Peck, H. Renata, F. H. Arnold, *Chem. Sci.* **2014**, *5*, 598–601.
[8] a) M. Bordeaux, V. Tyagi, R. Fasan, *Angew. Chem. Int. Ed.* **2015**, *54*, 1744–1748; *Angew. Chem.* **2015**, *127*, 1764–1768; b) G. Sreenilayam, R. Fasan, *Chem. Commun.* **2015**, *51*, 1532–1534; c) V. Tyagi, R. B. Bonn, R. Fasan, *Chem. Sci.* **2015**, *6*, 2488–2494.
[9] C. Lionetti, M. G. Guanziroli, F. Frigerio, P. Ascenzi, M. Bolognesi, *J. Mol. Biol.* **1991**, *217*, 409–412.
[10] R. A. Mcclelland, M. Coe, *J. Am. Chem. Soc.* **1983**, *105*, 2718–2725.
[11] R. L. Khade, W. C. Fan, Y. Ling, L. Yang, E. Oldfield, Y. Zhang, *Angew. Chem. Int. Ed.* **2014**, *53*, 7574–7578; *Angew. Chem.* **2014**, *126*, 7704–7708.
[12] a) E. Vedejs, K. A. J. Snoble, *J. Am. Chem. Soc.* **1973**, *95*, 5778–5780; b) P. A. Byrne, D. G. Gilheany, *Chem. Soc. Rev.* **2013**, *42*, 6670–6696.
[13] M. Bordeaux, R. Singh, R. Fasan, *Bioorg. Med. Chem.* **2014**, *22*, 5697–5704.
[14] D. Ringe, G. A. Petsko, D. E. Kerr, P. R. O. de Montellano, *Biochemistry* **1984**, *23*, 2–4.
[15] E. Vedejs, M. J. Peterson, *Topics in Stereochemistry*, *Vol. 21*, Wiley-VCH, Weinheim, **1994**.
[16] a) S. Ozaki, T. Matsui, Y. Watanabe, *J. Am. Chem. Soc.* **1997**, *119*, 6666–6667; b) J. Collot, J. Gradinaru, N. Humbert, M. Skander, A. Zocchi, T. R. Ward, *J. Am. Chem. Soc.* **2003**, *125*, 9030–9031; c) T. Ueno, T. Koshiyama, M. Ohashi, K. Kondo, M. Kono, A. Suzuki, T. Yamane, Y. Watanabe, *J. Am. Chem. Soc.* **2005**, *127*, 6556–6562; d) Y. W. Lin, N. Yeung, Y. G. Gao, K. D. Miner, S. L. Tian, H. Robinson, Y. Lu, *Proc. Natl. Acad. Sci. USA* **2010**, *107*, 8581–8586; e) C. Mayer, D. G. Gillingham, T. R. Ward, D. Hilvert, *Chem. Commun.* **2011**, *47*, 12068–12070; f) J. Bos, F. Fusetti, A. J. M. Driessen, G. Roelfes, *Angew. Chem. Int. Ed.* **2012**, *51*, 7472–7475; *Angew. Chem.* **2012**, *124*, 7590–7593; g) T. K. Hyster, L. Knorr, T. R. Ward, T. Rovis, *Science* **2012**, *338*, 500–503; h) X. Liu, Y. Yu, C. Hu, W. Zhang, Y. Lu, J. Wang, *Angew. Chem. Int. Ed.* **2012**, *51*, 4312–4316; *Angew. Chem.* **2012**, *124*, 4388–4392; i) R. Singh, M. Bordeaux, R. Fasan, *ACS Catal.* **2014**, *4*, 546–552; j) R. Singh, J. N. Kolev, P. A. Sutera, R. Fasan, *ACS Catal.* **2015**, *5*, 1685–1691; k) S. Giovani, R. Singh, R. Fasan, *Chem. Sci.* **2016**, *7*, 234–239; l) T. K. Hyster, C. C. Farwell, A. R. Buller, J. A. McIntosh, F. H. Arnold, *J. Am. Chem. Soc.* **2014**, *136*, 15505–15508; m) C. C. Farwell, J. A. McIntosh, T. K. Hyster, Z. J. Wang, F. H. Arnold, *J. Am. Chem. Soc.* **2014**, *136*, 8766–8771; n) D. J. Sommer, M. D. Vaughn, G. Ghirlanda, *Chem. Commun.* **2014**, *50*, 15852–15855; o) P. Srivastava, H. Yang, K. Ellis-Guardiola, J. C. Lewis, *Nat. Commun.* **2015**, *6*, 7789; p) Y. Yu, C. Cui, X. Liu, I. D. Petrik, J. Wang, Y. Lu, *J. Am. Chem. Soc.* **2015**, *137*, 11570–11573.

Received: September 20, 2015
Revised: November 14, 2015
Published online: January 14, 2016

Angewandte Chemie
Eine Zeitschrift der Gesellschaft Deutscher Chemiker

Supporting Information

Myoglobin-Catalyzed Olefination of Aldehydes

*Vikas Tyagi and Rudi Fasan**

anie_201508817_sm_miscellaneous_information.pdf

Table of contents:

Supplementary Figure S1. Crystal structure of wild-type sperm whale myoglobin (pdb 1A6K). Residues targeted for mutagenesis (**Figure 1**) are highlighted in blue and displayed as stick models. The heme cofactor is colored in yellow.

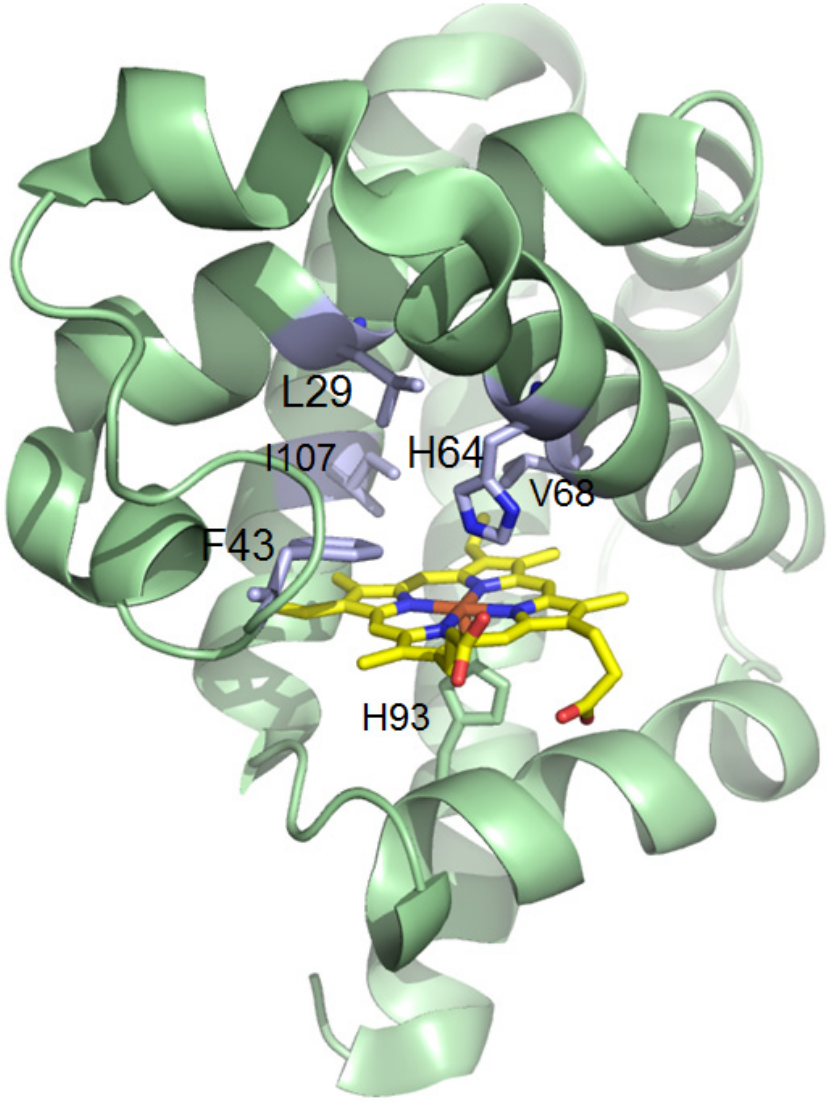

Supplementary Figure S2: Time-course analysis of Mb(F43V,V68F)-catalyzed formation of ethyl cinnamate (**3a**) from benzaldehyde (**1**) in the presence of triphenylarsine and EDA (**2a**). Conversion was determined by gas chromatography using calibration curves with isolated **3a**. Reaction conditions: 1 μM Mb(F43V,V68F), 10mM benzaldehyde, 10 mM triphenylarsine, 10 mM EDA, 10 mM dithionite in oxygen-free phosphate buffer (pH 8.0).

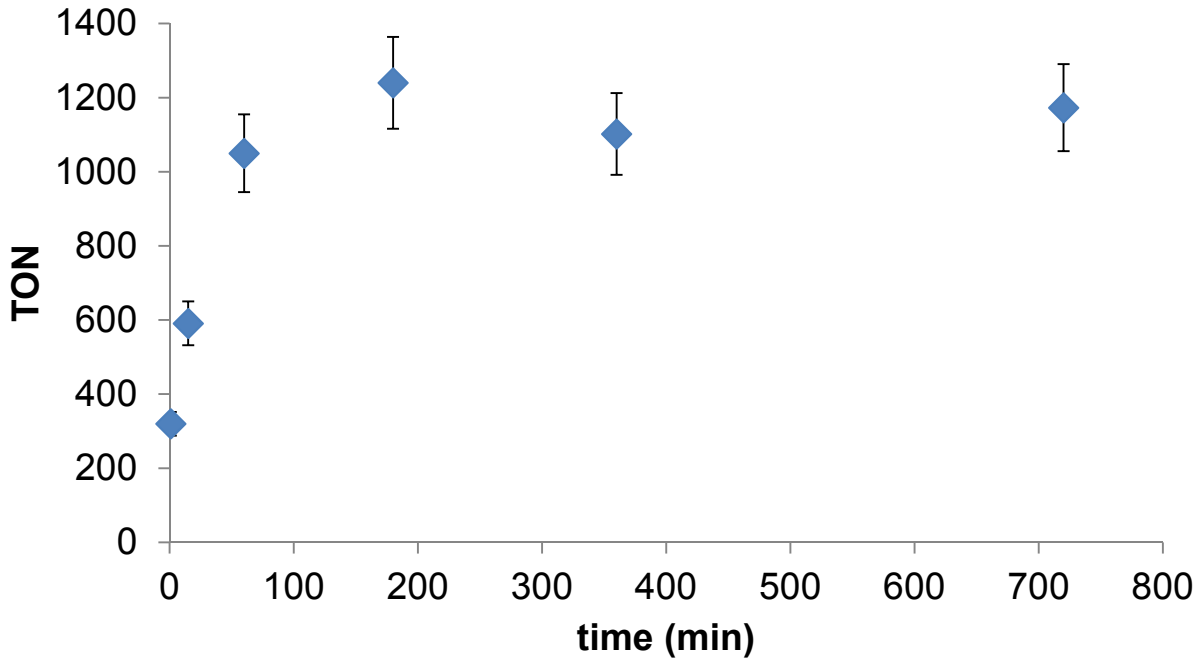

Supplementary Figure S3: Product inhibition effects inMb(F43V,V68F)-catalyzed conversion of benzaldehyde (**1**) to ethyl cinnamate (**3a**) in the presence of $AsPh_3$ and EDA. The reaction mixtures (1 μM Mb(F43V,V68F), 10 mM benzaldehyde, 10 mM $AsPh_3$, 10 mM EDA, 10 mM dithionite in oxygen-free phosphate buffer at pH 8.0) were added with increasing amounts ofethyl cinnamate or phosphine oxide (0-10 mM). TON values were determined by GC and normalized to TON values in the absence of added ethyl cinnamate or phosphine oxide.

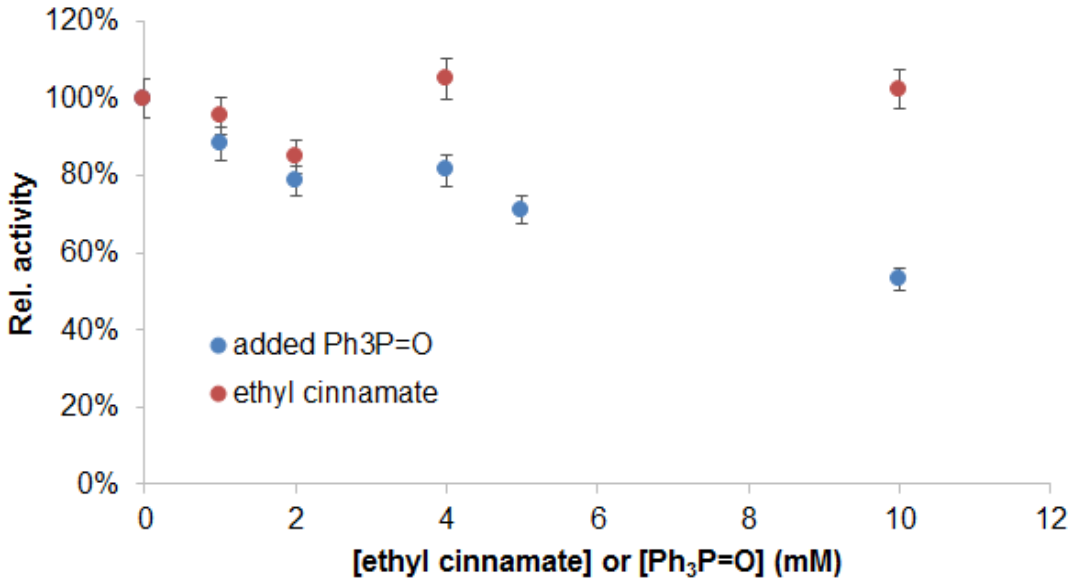

Experimental Procedures

Reagents and Analytical Methods. All the chemicals and reagents were purchased from commercial suppliers (Sigma-Aldrich, Alfa Aesar) and used without any further purification, unless otherwise stated. All dry reactions were carried out under argon atmosphere in oven-dried glassware with magnetic stirring using standard gas-tight syringes, cannulae and septa. ^{1}H and ^{13}C NMR spectra were measured on Bruker DPX-400 (operating at 400 MHz for ^{1}H and 100 MHz for ^{13}C) or Bruker DPX-500 (operating at 500 MHz for ^{1}H and 125 MHz for ^{13}C). Tetramethylsilane (TMS) served as the internal standard (0 ppm) for ^{1}H NMR and $CDCl_3$ was used as the internal standard (77.0 ppm) for ^{13}C NMR. Silica gel chromatography purifications were carried out using AMD Silica Gel 60 230-400 mesh. Gas chromatography (GC) analyses were carried out using a Shimadzu GC-2010 gas chromatograph equipped with a FID detector and aChiral Cyclosil-B column (30 m x 0.25 mm x 0.25 μm film). Separation methodfor calculation of TON and TTN values: 1 μL injection, injector temp.: 200 ºC, detector temp: 300 ºC. Gradient: column temperature set at 80 ºC for 3 min, then to 160 ºC at 2.80 ºC/min, then to 165 ºC at 1 ºC/min, then to 245 ºC at 25 ºC/min. Total run time was 45.77 min.

Protein expression and purification. Wild-type Mb and the engineered Mb variants were expressed in *E. coli* BL21(DE3) cells as described previously (M. Bordeaux, V. Tyagi, R. Fasan, *Angew. Chem. Int. Ed.***2015**, 54, 1744–1748).Briefly, cells were grown in TB medium (ampicillin, 100 mg L^{-1}) at 37 °C (150 rpm) until OD_{600} reached 0.6. Cells were then induced with 0.25 mM β-D-1-thiogalactopyranoside (IPTG) and 0.3 mM δ-aminolevulinic acid (ALA). After induction, cultures were shaken at 150 rpm and 27 °C

and harvested after 20 h by centrifugation at 4000 rpm at 4 °C. After cell lysis by sonication, the proteins were purified by Ni-affinity chromatography using the following buffers: loading buffer (50 mM Kpi, 800 mM NaCl, pH 7.0), wash buffer 1 (50 mM Kpi, 800 mM NaCl, pH 6.2), wash buffer 2 (50 mM Kpi, 800 mM NaCl, 250 mM glycine, pH 7.0) and elution buffer (50 mM Kpi, 800 mM NaCl, 300 mM L-histidine, pH 7.0). After buffer exchange (50 mM Kpi, pH 7.0), the proteins were stored at +4 °C. Myoglobin concentration was determined using an extinction coefficient ε_{410} = 157 mM^{-1} cm^{-1}.[2]

Aldehyde olefination reaction. Initial reactions (**Table 1**) were carried out at a 400 µL scale using 20 µM myoglobin, 10 mM benzaldehyde, 10 mM EDA, 10 mM triphenylphosphine (or trialkyl phosphines, $AsPh_3$, $SbPh_3$, $BiPh_3$) and 10 mM sodium dithionite. In a typical procedure, a solution containing sodium dithionate (100 mM stock solution) in potassium phosphate buffer (50 mM, pH 8.0) was degassed by bubbling argon into the mixture for 4 min in a sealed vial. A buffered solution containing myoglobin was carefully degassed in a similar manner in a separate vial. The two solutions were then mixed together via cannula. Reactions were initiated by addition of 10 µL of benzaldehyde (from a 0.4 M stock solution in DMSO), 10 µL triphenylphosphine (from a 0.4 M stock solution in DMSO) of followed by the addition of 10µL of EDA (from a 0.4 M stock solution in DMSO) with a syringe, and the reaction mixture was stirred for 12 h at room temperature, under positive argon pressure. For the optimization of the benzaldehyde: triphenylarsine:EDA ratio, reactions were performed according to the general procedure described above, using 20 µM of protein, 10 mM of benzaldehyde and variable amounts of triphenylarsine and EDA (5 mM EDA to 20mM EDA). Optimization of the substrate loading was done in a similar manner, using 20 µM

Mb, variable quantities of benzaldehyde (from 1 to 40mM final concentration), and variable quantities of triphenylarsine and EDA (from 1 to 40 mM final concentration), maintaining an benzaldehyde: triphenylarsine: EDA ratio of 1:1:1 at all times. Enzyme concentration optimization was carried according to the general procedure along with varying the enzyme concentration from 20 μM to 1 μM of Mb(F43V V68F)and 10 mM benzaldehyde (10 μL of 0.4 M stock solution in DMSO), 10 mM triphenylarsine (10 μL of 0.4 M stock solution in DMSO) and 10 mM EDA (10 μL of 0.4 M stock solution in DMSO). Reactions for TON determination were carried out according to the general procedure described above using 1 μM Mb(F43V V68F), benzaldehyde (10 μL of 0.4 M stock solution in DMSO), 10 mM triphenylarsine (10 μL of 0.4 M stock solution in DMSO) and 10 mM EDA (10 μL of 0.4 M stock solution in DMSO).

Product analysis. The reactions were analyzed by adding 20 μL of internal standard (benzodioxole, 50 mM in methanol) to the reaction mixture, followed by extraction with 400 μL of dichloromethane and separated organic layer was analyzed by GC-FID (see **Reagents and Analytical Methods** section for details on GC analyses). Calibration curves for quantification of the different aldehyde olefination products were constructed using authentic standards prepared synthetically as described in **Synthetic Procedures**. Benzyl cinnamate (**3c**) was purchased from Sigma-Aldrich. All measurements were performed at least in duplicate. For each experiment, negative control samples containing either no enzyme or no reductant were included.

Synthetic Procedures:

Synthesis of authentic ethyl cinnamate and *tert*-butyl cinnamate products (procedure 1):

To a flame dried round bottom flask under argon, equipped with a stir bar was added aryl aldehydes (1 equiv.), triphenylphosphine (1.5 equiv.), and Fe(TPP)Cl (1.5 mol%) in toluene (4-5 mL). A solution of EDA or *t*-BDA (1.5 equiv) in 2-3 mL of toluene was added dropwise over approximately 5 min. The resulting mixture was stirred at 80^{o}C for overnight. The solvent was removed under vacuum and the crude mixture was purified by 9:1 hexanes to diethyl ether using flash chromatography to obtained aryl substituted ethyl cinnamate or *tert*-butyl cinnamate products. The identity of the ethyl cinnamate or *tert*-butyl cinnamate products was determined using GC-MS, ^{1}H and ^{13}C NMR.

Synthesis of authentic standard for aryl substituted cyclohexyl cinnamate products (procedure 2):

To a flame dried round bottom flask under argon, equipped with a stir bar was added cinnamic acid (1 equiv.) and the cyclohexanol (1.2 equiv.) in THF (10 mL). After addition of DCC (1.2 equiv.) and DMAP (catalytic amount), the resulting mixture was stirred at room temperature until complete disappearance of the starting material. After evaporation and column chromatography on silica gel in 9:1 hexanes to diethyl ether using flash chromatography the desired product was obtained.

Compound Characterization Data:

Ethyl cinnamate (3a)

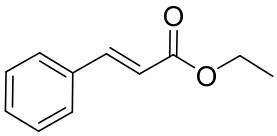

Following the standard procedure 1, 89% yield, GC-MS m/z (% relative intensity): 176(29.0), 148(15.9), 131(100), 103(48.3); ^{1}H NMR ($CDCl_3$, 500 MHz): δ 7.70 (d, J = 16 Hz, 1H), 7.51-7.50 (m, 2H), 7.37-7.36 (m, 3H), 6.45 (d, J = 16 Hz, 1H), 4.28 (q, J = 7.0 Hz, 2H), 1.34 (t, J = 7.0 Hz, 3H) ppm, ^{13}C NMR ($CDCl_3$, 125 MHz): δ 166.9, 144.5, 134.5, 130.2, 128.8, 128.0, 118.3, 60.4, 14.3 ppm.

Cyclohexyl cinnamate (3b)

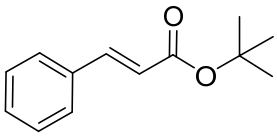

Following the standard procedure 1, 72% yield, GC-MS m/z (% relative intensity): 204(7.9), 147(100), 131(65.2), 103(31.8); ^{1}H NMR ($CDCl_3$, 500 MHz): δ 7.61 (d, J =16 Hz, 1H), 7.50-7.49 (m, 2H), 7.36-7.35 (m, 3H), 6.39 (d, J = 16 Hz, 1H), 1.54 (s, 9H) ppm, ^{13}C NMR ($CDCl_3$, 125 MHz): δ 166.3, 143.5, 134.7, 129.9, 128.8, 127.9, 120.2, 80.4, 28.2 ppm.

Cyclohexyl cinnamate (3d)

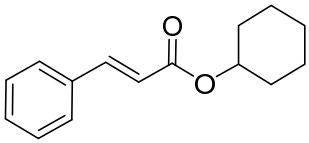

Following the standard procedure 2, 86% yield, GC-MS m/z (% relative intensity): 230(3.6), 149(37.7), 131(100), 103(38.7); ^{1}H NMR ($CDCl_3$, 400 MHz): δ 7.69 (d, J = 16.0

Hz, 1H), 7.51-7.50 (m, 2H) 7.37-7.35 (m, 3H), 6.45 (d, J = 16 Hz, 1H), 4.92-4.87 (m, 1H), 1.92-1.91 (m, 2H), 1.78-1.75 (m, 2H), 1.58-1.27 (m, 6H) ppm, ^{13}C NMR ($CDCl_3$, 100 MHz): δ 166.1, 144.0, 134.3, 129.8, 128.6, 127.7, 118.7, 72.4, 31.5, 25.2, 23.6 ppm.

(E)-Cyclohexyl 3-(o-tolyl)acrylate (5b)

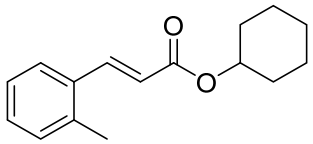

Following the standard procedure 2, 68% yield, GC-MS m/z (% relative intensity): 244(5.7), 162(28.1), 145(100), 116(68.4); ^1H NMR ($CDCl_3$, 400 MHz): δ 7.98 (d, J = 16 Hz 1H), 7.55 (d, J = 7.5 Hz, 1H), 7.26-7.17 (m, 3H), 6.37 (d, J = 16 Hz, 1H), 4.92-4.88 (m, 1H), 2.43 (s, 3H), 1.92-1.76 (m, 2H), 1.58-1.55 (m, 2H), 1.54-1.31 (m, 6H) ppm, ^{13}C NMR ($CDCl_3$, 100 MHz): δ 166.5, 141.9, 137.5, 133.5, 130.7, 129.8, 126.4, 126.3, 119.9, 72.6, 31.7, 25.5, 23.8, 19.7 ppm.

(E)-Cyclohexyl 3-(4-methyl-phenyl)acrylate (6b)

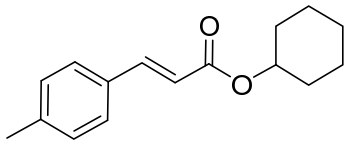

Following the standard procedure 2, 70% yield, GC-MS m/z (% relative intensity): 246(13.0), 164(100), 147(69.4), 120(18.4); ^1H NMR ($CDCl_3$, 400 MHz): δ 7.66 (d, J = 15.6 Hz, 1H), 7.42 (d, J = 6.0 Hz, 2H), 7.18 (d, J = 5.6 Hz, 2H), 6.40 (d, J = 15.6 Hz, 1H), 4.89-4.88 (m, 1H), 2.36 (s, 3H), 2.00 (m, 2H), 1.90 (m, 2H), 1.58-1.26 (m, 6H) ppm, ^{13}C NMR ($CDCl_3$, 100 MHz): δ 166.4, 144.0, 140.2, 131.6, 129.3, 127.7, 117.6, 72.4, 31.5, 25.2, 23.6, 21.2 ppm.

(E)-Cyclohexyl 3-(4-methoxy-phenyl)acrylate (7b)

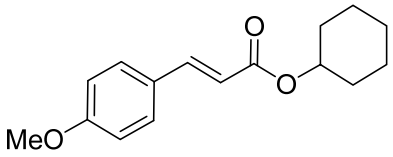

Following the standard procedure 2, 71% yield, GC-MS m/z (% relative intensity): 260(25.4), 178(100), 161(74.8), 134(42.8); ^{1}H NMR ($CDCl_3$, 400 MHz): δ 7.64 (d, J = 16 Hz, 1H), 7.48 (d, J = 8.4 Hz, 2H), 6.90 (d, J = 8.4 Hz, 2H), 6.32 (d, J = 16 Hz, 1H), 4.90-4.84 (m, 1H), 3.82 (s, 3H), 1.91-1.90 (m, 2H), 1.78-1.75 (m, 2H), 1.58-1.27 (m, 6H) ppm, ^{13}C NMR ($CDCl_3$, 100 MHz): δ 166.5, 161.0, 143.6, 129.4, 127.1, 116.2, 114.0, 72.2, 55.1, 31.5, 25.2, 23.6 ppm.

(E)-Cyclohexyl 3-(4-fluoro-phenyl)acrylate (8b)

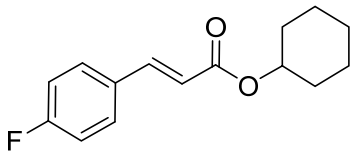

Following the standard procedure 2, 62% yield, GC-MS m/z (% relative intensity): 248(3.1), 166(61.9), 149(100), 28.8(121), 101(30.5); ^{1}H NMR ($CDCl_3$, 400 MHz): δ 7.64 (d, J = 16 Hz, 1H), 7.51-7.48 (m, 2H), 7.08-7.04 (m, 2H), 6.37 (d, J = 16 Hz, 1H), 4.89-4.86 (m, 1H), 1.91-1.89 (m, 2H), 1.76-1.75 (m, 2H), 1.57-1.25 (m, 6H) ppm, ^{13}C NMR ($CDCl_3$, 100 MHz): δ 166.0, 142.7, 130.6, 129.6, 129.5, 118.4, 115.8, 115.6, 72.5, 31.5, 25.2, 23.6 ppm.

(E)-Cyclohexyl 3-(4-chloro-phenyl)acrylate (9b)

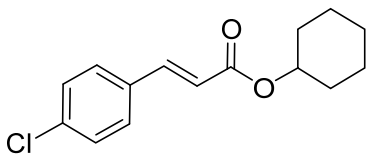

Following the standard procedure 2, 76% yield, GC-MS m/z (% relative intensity): 264(5.7), 182(86.8), 165(100), 137(33.1), 102(42.0); ^{1}H NMR ($CDCl_3$, 400 MHz): δ 7.62 (d, J =16 Hz, 1H), 7.46 (d, J = 8.4 Hz, 2H), 7.36 (d, J = 7.6 Hz, 2H), 6.42 (d, J = 16 Hz,

1H), 4.90-4.86 (m, 1H), 1.91-1.90 (m, 2H), 1.78-1.75 (m, 2H), 1.56-1.25 (m, 6H) ppm, ^{13}C NMR ($CDCl_3$, 100 MHz): δ 165.9, 142.5, 135.7, 132.8, 129.0, 128.9, 119.2, 72.7, 31.5, 25.2, 23.6 ppm.

(E)-Cyclohexyl 3-(4-bromo-phenyl)acrylate (10b)

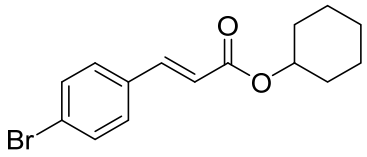

Following the standard procedure 2, 82% yield, GC-MS m/z (% relative intensity): 308(4.1), 226(73.1), 209(59.5), 102(100); ^1H NMR ($CDCl_3$, 400 MHz): δ 7.61(d, J = 16 Hz, 1H), 7.51 (d, J = 8.4 Hz, 2H), 7.39 (d, J = 8.4 Hz, 2H), 6.43 (d, J = 16 Hz, 1H), 4.90-4.85 (m, 1H), 1.91-1.90 (m, 2H), 1.78-1.75 (m, 2H), 1.60-1.25 (m, 6H) ppm, ^{13}C NMR ($CDCl_3$, 100 MHz): δ 165.9, 142.6, 133.2, 131.8, 129.1, 124.1, 119.4, 72.6, 31.5, 25.2, 23.5 ppm.

(E)-Cyclohexyl 3-(4-(trifluoromethyl)phenyl)acrylate (11b)

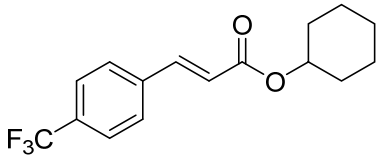

Following the standard procedure 2, 72% yield, GC-MS m/z (% relative intensity):217(73.8), 199(100), 171(30.4), 151(45.7);^1H NMR ($CDCl_3$, 400 MHz): δ 7.69-7.63 (m, 5H), 6.52 (d, J = 16 Hz, 1H), 4.90 (m, 1H), 1.91 (m, 2H), 1.76 (m, 2H), 1.58-1.25 (m, 6H) ppm, ^{13}C NMR ($CDCl_3$, 100 MHz): δ 165.6, 142.1, 137.7, 127.8, 125.5, 121.3, 72.9, 31.5, 25.1, 23.5 ppm.

(E)-Cyclohexyl 3-(4-nitro-phenyl)acrylate (12b)

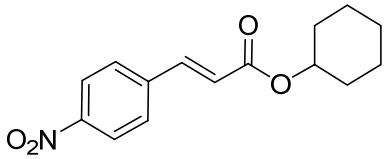

Following the standard procedure 2, 55% yield, GC-MS m/z (% relative intensity): 194(85.8), 176(100), 130(37.9), 102(44.1); ^{1}H NMR ($CDCl_3$, 400 MHz): δ 8.24 (d, J = 7.2 Hz, 2H), 7.70-7.65 (m, 3H), 6.57 (d, J = 16 Hz, 1H), 4.91-4.90 (m, 1H), 1.90 (m, 2H), 1.75 (m, 2H), 1.58-1.25 (m, 6H) ppm, ^{13}C NMR ($CDCl_3$, 100 MHz): δ 165.2, 148.2 141.0, 140.5, 128.3, 123.9, 123.0, 73.1, 31.4, 25.1, 23.5 ppm.

(E)-Cyclohexyl 3-(4-(dimethylamino)-phenyl)acrylate (13b)

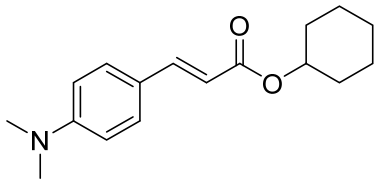

Following the standard procedure 2, 62% yield, GC-MS m/z (% relative intensity):273(54.9), 191(100), 174(34.2), 147(49.9); ^{1}H NMR ($CDCl_3$, 400 MHz): δ 7.62 (d, J = 15.6 Hz, 1H), 7.42 (d, J = 8.8 Hz, 2H), 6.66 (d, J = 8.4 Hz, 2H), 6.23 (d, J = 15.6 Hz, 1H), 4.89-4.84 (m, 1H), 2.99 (s, 6H), 1.92-1.91 (m, 2H), 1.78-1.76 (m, 2H), 1.58-1.26 (m, 6H) ppm, ^{13}C NMR ($CDCl_3$, 100 MHz): δ 167.1, 151.4, 144.6, 129.4, 122.1, 112.9, 111.5, 71.9, 39.9, 31.6, 25.2, 23.7 ppm.

(E)-Cyclohexyl 3-(2,5-dimethylphenyl)acrylate (14b)

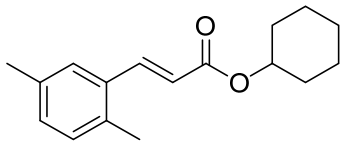

Following the standard procedure 2, 60% yield, GC-MS m/z (% relative intensity): 258(17.6), 176(52.8), 159(100), 130(94.9), 115(44.6);^{1}H NMR ($CDCl_3$, 400 MHz): δ 7.96

(d, J = 16 Hz, 1H), 7.35 (s, 1H), 7.05 (s, 2H), 6.37 (d, J = 15.6 Hz, 1H), 4.94-4.87 (m, 1H), 2.37 (s, 3H), 2.30 (s, 3H), 1.93-1.91 (m, 2H), 1.79-1.76 (m, 2H), 1.58-1.27 (m, 6H) ppm, ^{13}C NMR ($CDCl_3$, 100 MHz): δ 166.2, 141.9, 141.8, 135.3, 134.3, 132.9, 130.5, 130.4, 126.6, 119.2, 72.3, 31.5, 25.3, 23.6 ppm.

(E)-Ethyl 3-(naphthalen-2-yl)acrylate (15b)

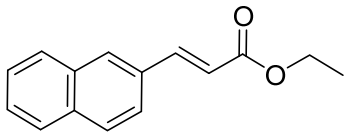

Following the standard procedure 2, 82% yield, GC-MS m/z (% relative intensity): 226(73.3), 198(14.7), 181(100), 152(92.5); ^{1}H NMR ($CDCl_3$, 500 MHz): δ 7.85-7.75 (m, 4H), 7.61 (d, J = 8.5 Hz, 1H), 7.49-7.45 (m, 2H), 6.55 (d, J = 16 Hz, 1H), 4.33 (q, J = 7.0 Hz, 2H), 1.38 (t, J = 7.0 Hz, 3H) ppm, ^{13}C NMR ($CDCl_3$, 125 MHz): δ 167.0, 144.6, 134.2, 133.3, 131.9, 129.9, 128.6, 128.5, 127.8, 127.2, 126.7, 123.5, 118.4, 60.5, 14.4 ppm.

(E)-Ethyl 3-(thiophen-2-yl)acrylate (16b)

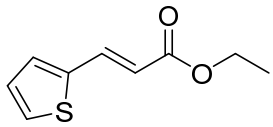

Following the standard procedure 2, 75% yield, GC-MS m/z (% relative intensity): 182(35.4), 154(11.5), 137(100), 109(40.1);^{1}H NMR ($CDCl_3$, 500 MHz): δ 7.76 (d, J = 15.5 Hz, 1H), 7.32 (d, J = 4.5 Hz, 1H), 7.20 (d, J = 3.0 Hz, 1H), 7.01-6.99 (m, 1H), 6.22 (d, J = 15.5 Hz, 1H), 4.23 (q, J = 7.0 Hz, 2H), 1.30 (t, J = 7.5 Hz, 3H) ppm, ^{13}C NMR ($CDCl_3$, 125 MHz): δ 166.7, 139.5, 136.9, 130.8, 128.3, 128.0, 117.0, 60.4, 14.3 ppm.

(E)-Ethyl 4-phenylbut-2-enoate (17b)

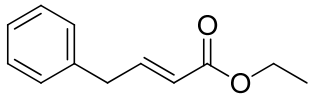

Following the standard procedure, % yield (67), GC-MS m/z (% relative intensity): 190(40.8), 145(39.0), 127(18.7), 117(100);^{1}H NMR ($CDCl_3$, 500 MHz): δ 7.33(t, J = 7.0 Hz, 2H), 7.26(t, J =7.5 Hz, 1H), 7.19 (d, J = 7.5 Hz, 2H), 7.14-7.08 (m, 1H), 5.84 (d, J = 15.5 Hz, 1H), 4.21(q, J = 7.0Hz, 2H), 3.53 (d, J = 6.5 Hz, 2H), 1.29 (t, J = 7.0 Hz, 3H) ppm, ^{13}C NMR ($CDCl_3$, 125 MHz): δ 166.4, 147.3, 137.7, 128.8, 128.7, 126.6, 122.4, 60.2, 38.4, 14.3 ppm.

^{1}H and ^{13}C NMR spectra:

3a:

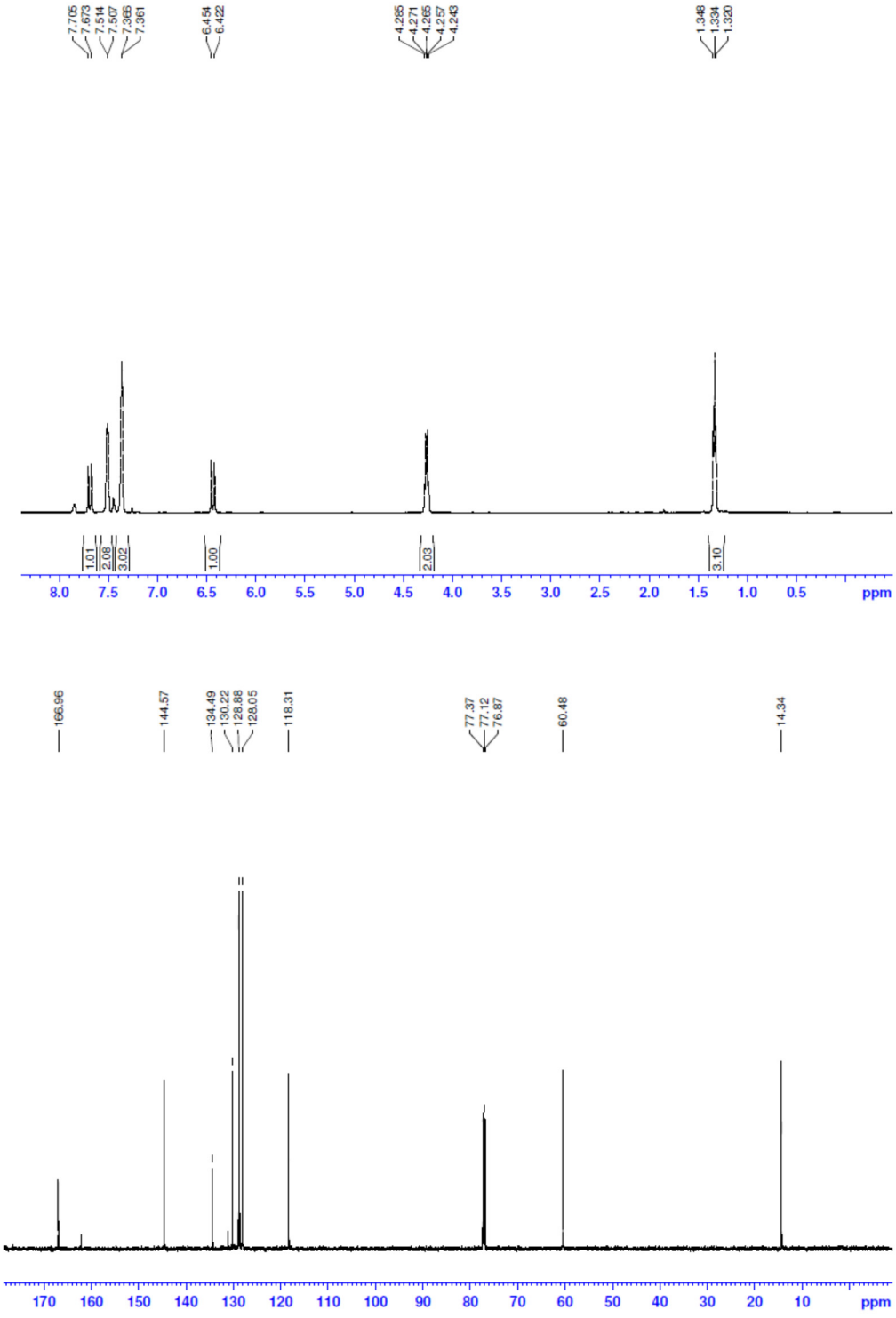

3b:

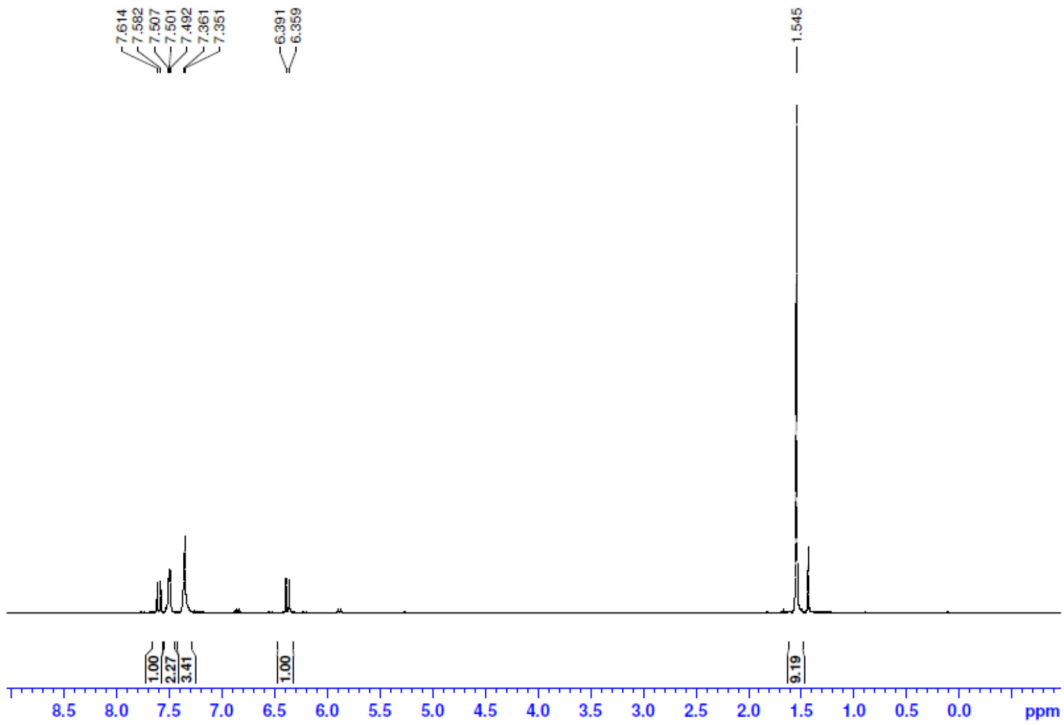
7.614
7.582
7.507
7.501
7.492
7.361
7.351
6.391
6.359
1.545
1.00
2.27
3.41
1.00
9.19
8.5 8.0 7.5 7.0 6.5 6.0 5.5 5.0 4.5 4.0 3.5 3.0 2.5 2.0 1.5 1.0 0.5 0.0 ppm

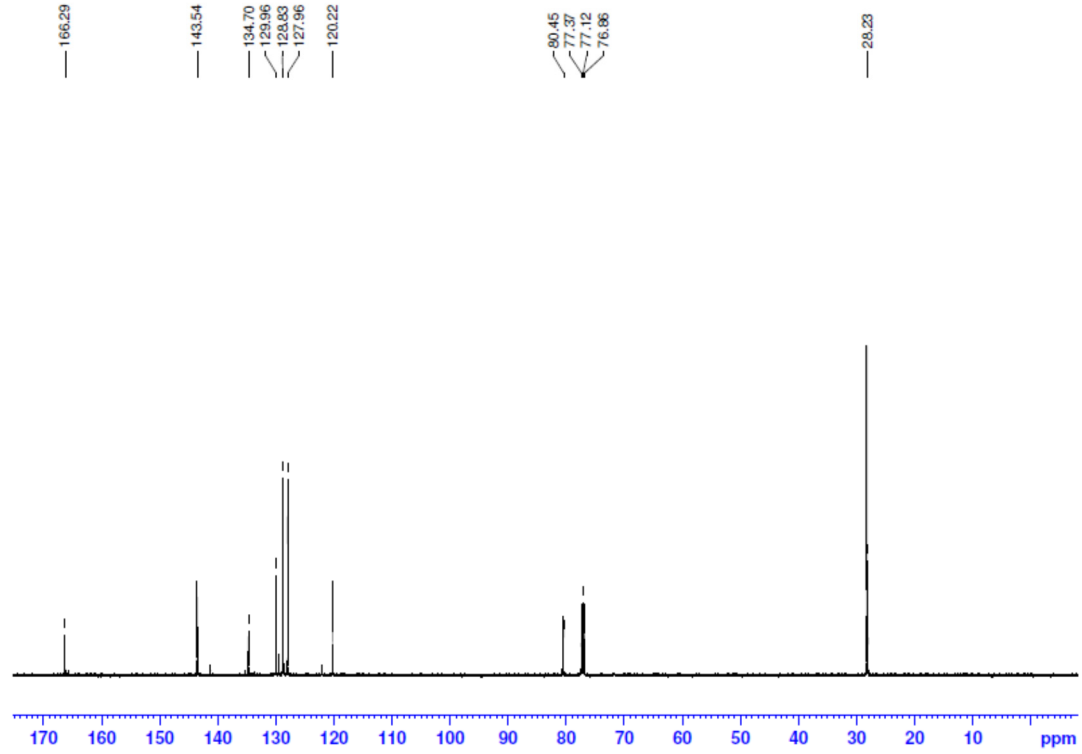
166.29
143.54
134.70
129.96
128.83
127.96
120.22
80.45
77.37
77.12
76.86
28.23
170 160 150 140 130 120 110 100 90 80 70 60 50 40 30 20 10 ppm

3d:

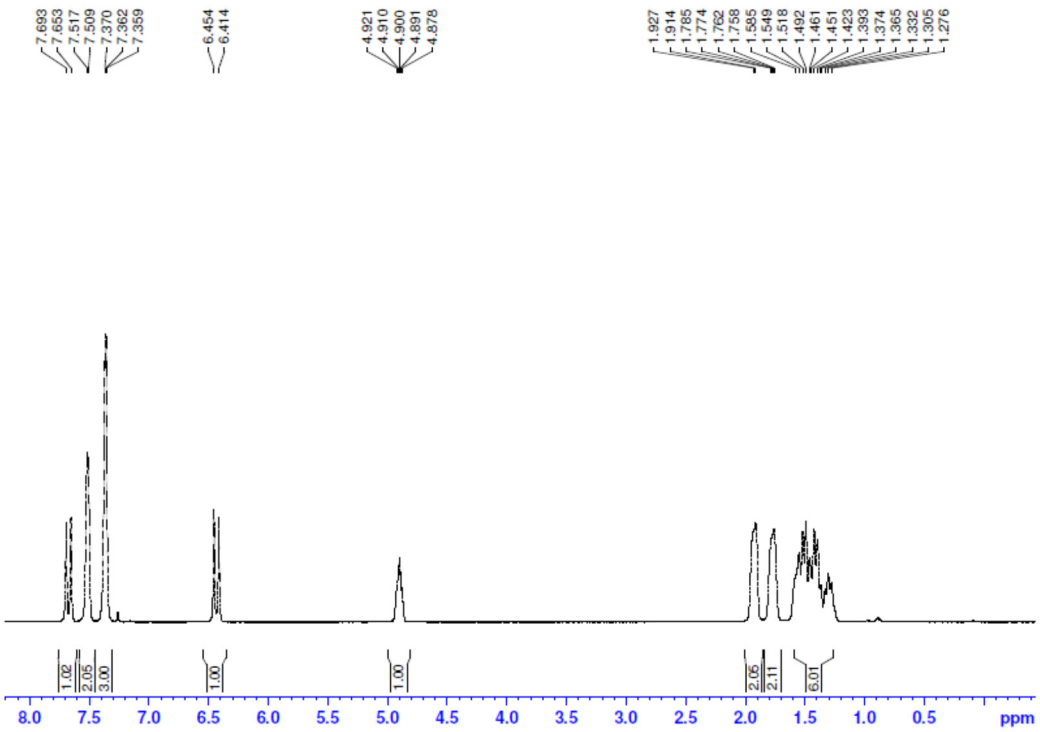
7.693
7.653
7.517
7.509
7.370
7.362
7.359
6.454
6.414
4.921
4.910
4.900
4.891
4.878
1.927
1.914
1.785
1.774
1.762
1.758
1.585
1.549
1.518
1.492
1.461
1.451
1.423
1.393
1.374
1.365
1.332
1.305
1.276
1.02
2.05
3.00
1.00
1.00
2.06
2.11
6.01
8.0
7.5
7.0
6.5
6.0
5.5
5.0
4.5
4.0
3.5
3.0
2.5
2.0
1.5
1.0
0.5
ppm

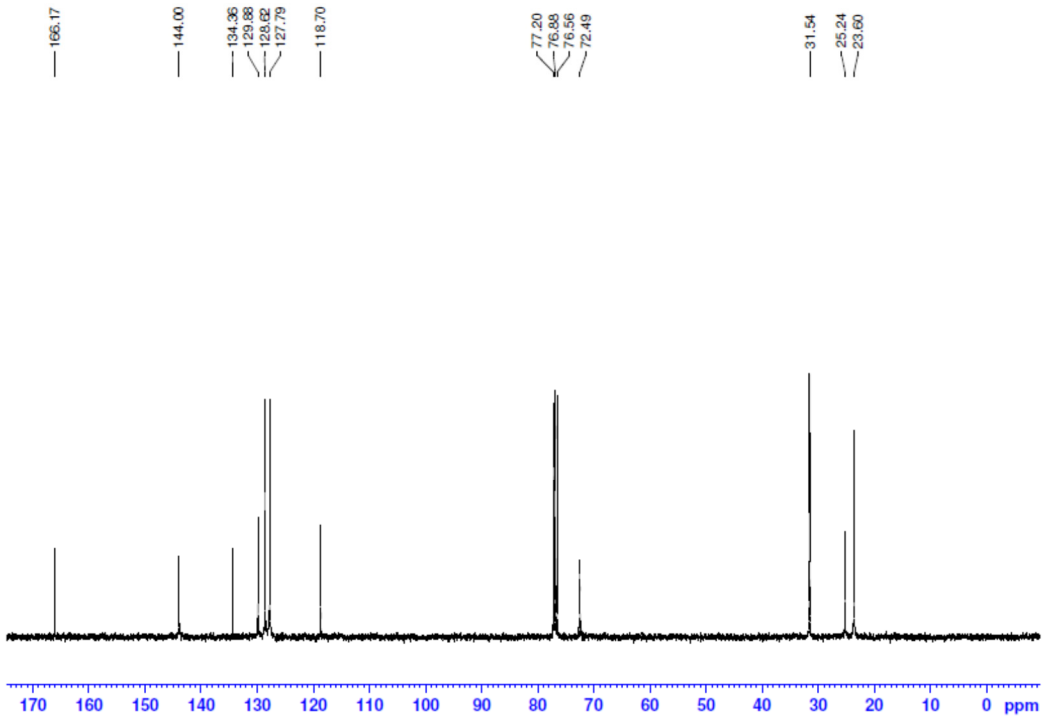
166.17
144.00
134.36
129.88
128.62
127.79
118.70
77.20
76.88
76.56
72.49
31.54
25.24
23.60
170
160
150
140
130
120
110
100
90
80
70
60
50
40
30
20
10
0
ppm

5b:

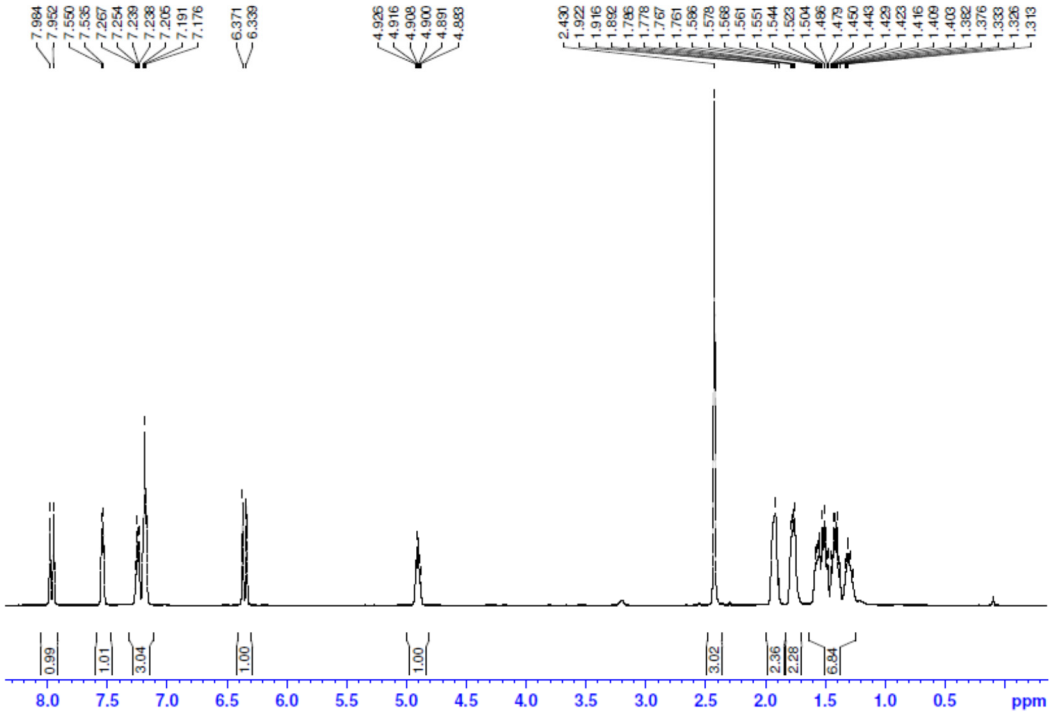
7.984
7.952
7.550
7.535
7.267
7.254
7.239
7.238
7.205
7.191
7.176
6.371
6.339
4.926
4.916
4.908
4.900
4.891
4.883
2.430
1.922
1.916
1.892
1.785
1.778
1.767
1.761
1.566
1.578
1.568
1.561
1.551
1.544
1.523
1.504
1.486
1.479
1.450
1.443
1.429
1.423
1.416
1.409
1.403
1.382
1.376
1.333
1.326
1.313
0.99
1.01
3.04
1.00
1.00
3.02
2.36
2.28
6.84
8.0
7.5
7.0
6.5
6.0
5.5
5.0
4.5
4.0
3.5
3.0
2.5
2.0
1.5
1.0
0.5
ppm

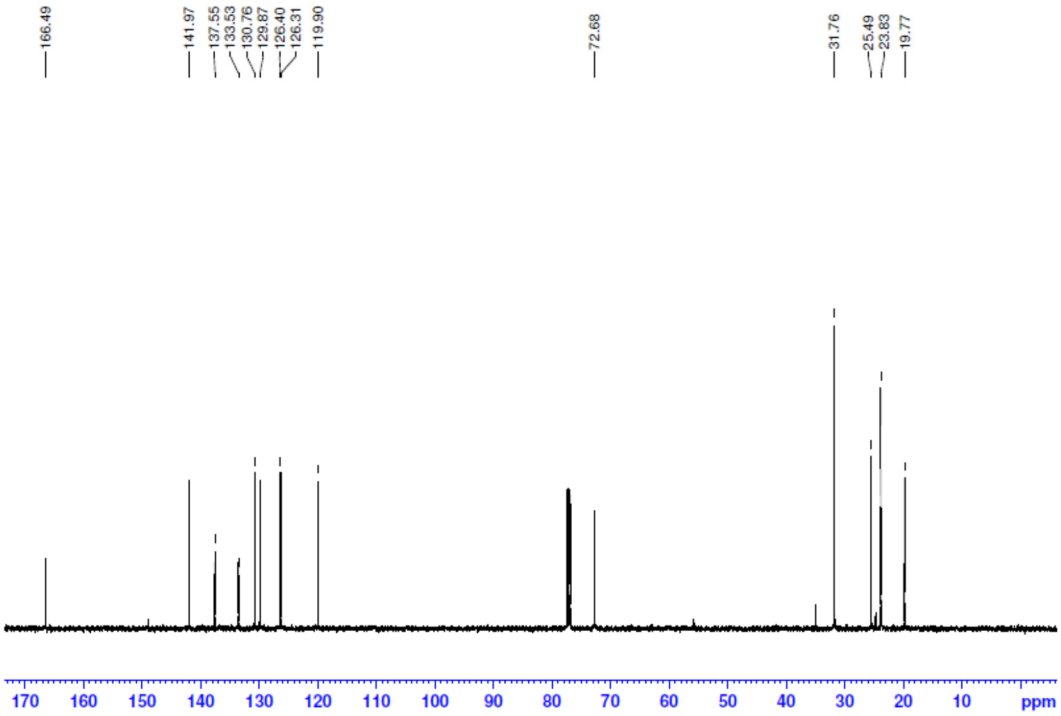
166.49
141.97
137.55
133.53
130.76
129.87
126.40
126.31
119.90
72.68
31.76
25.49
23.83
19.77
170
160
150
140
130
120
110
100
90
80
70
60
50
40
30
20
10
ppm

6b:

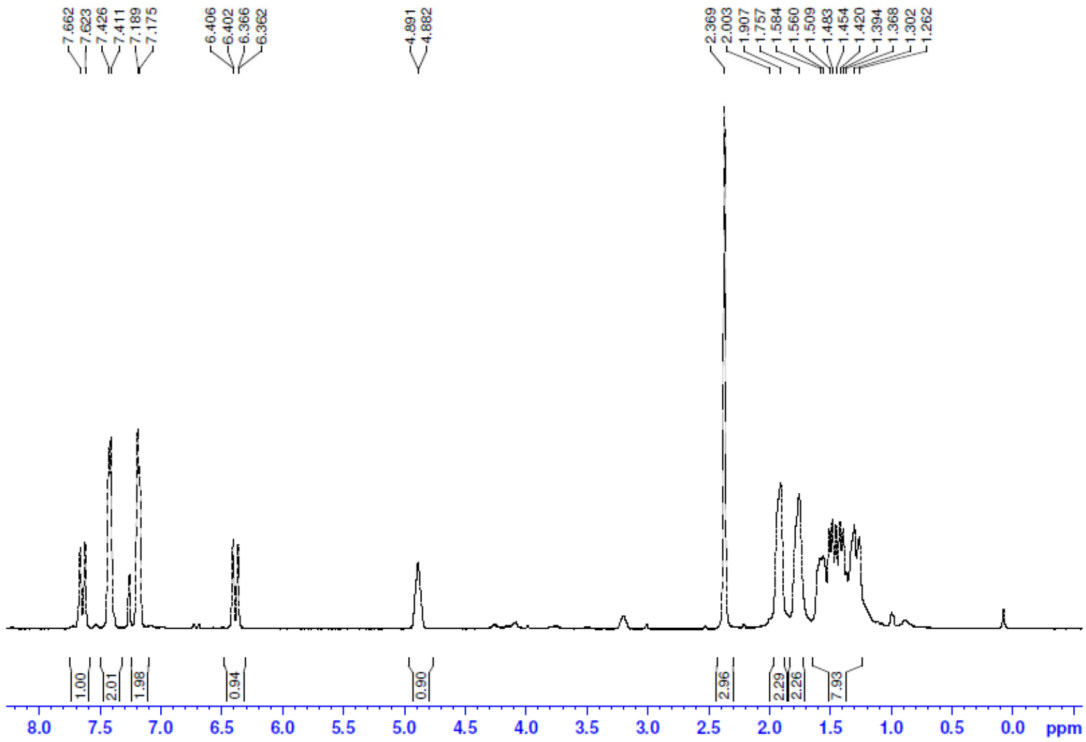
7.662
7.623
7.426
7.411
7.189
7.175
6.406
6.402
6.366
6.362
4.891
4.882
2.369
2.003
1.907
1.757
1.584
1.560
1.509
1.483
1.454
1.420
1.394
1.368
1.302
1.262
1.00
2.01
1.98
0.94
0.90
2.96
2.29
2.26
7.93
8.0
7.5
7.0
6.5
6.0
5.5
5.0
4.5
4.0
3.5
3.0
2.5
2.0
1.5
1.0
0.5
0.0
ppm

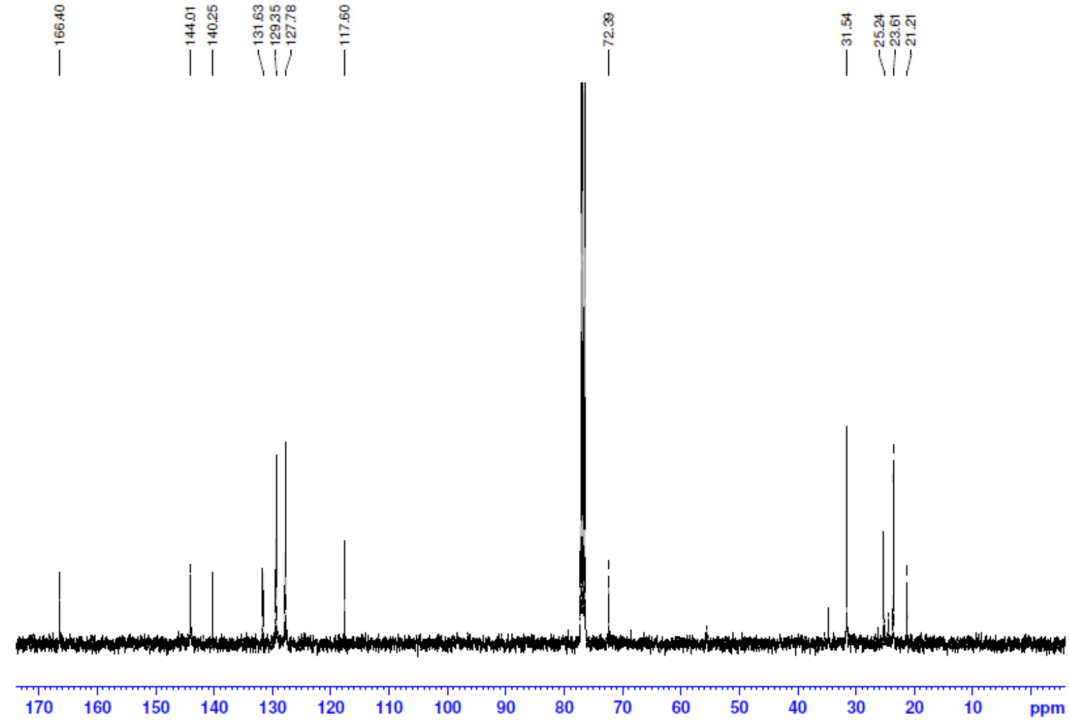
166.40
144.01
140.25
131.63
129.35
127.78
117.60
72.39
31.54
25.24
23.61
21.21
170
160
150
140
130
120
110
100
90
80
70
60
50
40
30
20
10
ppm

7b:

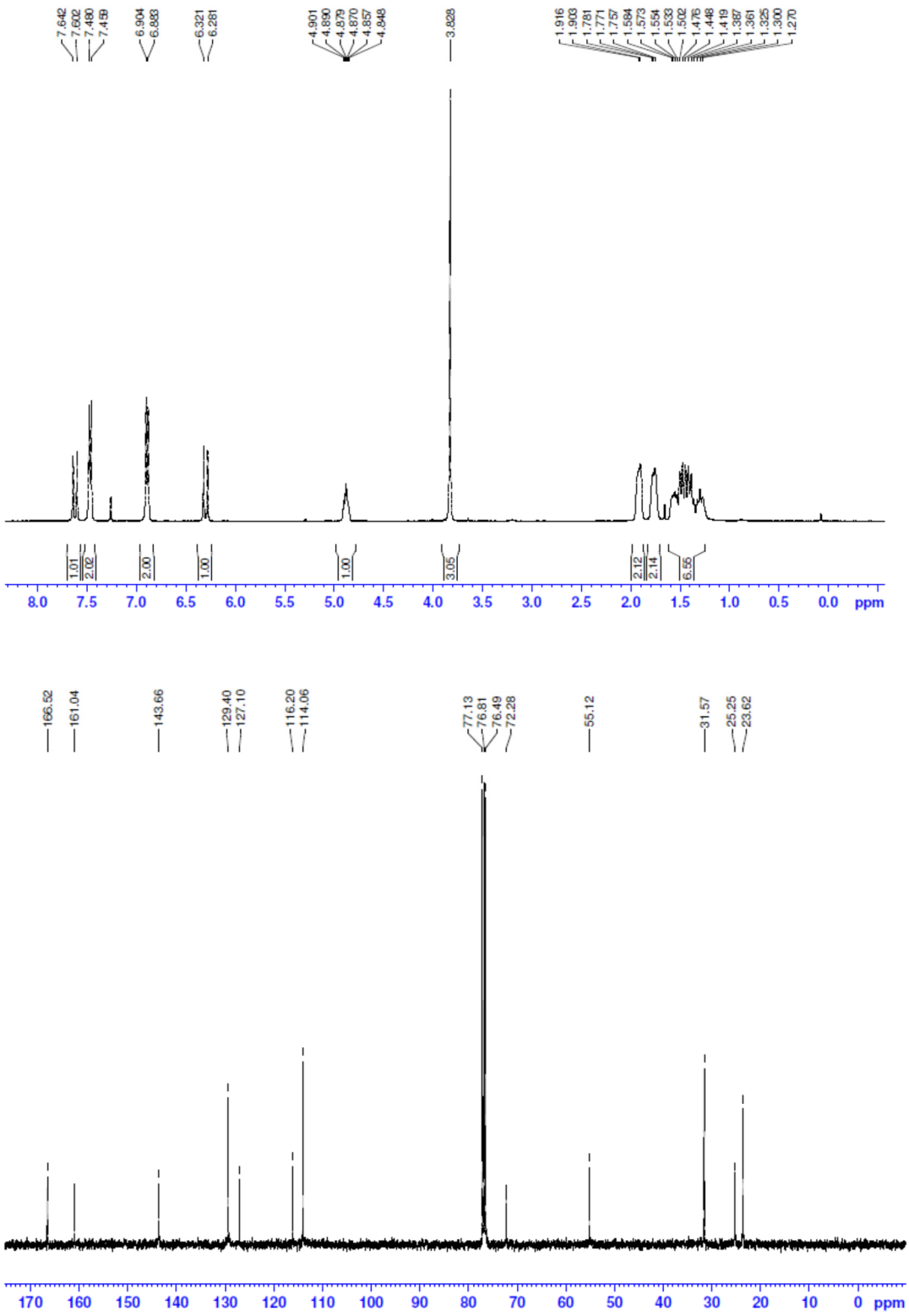
7.642
7.602
7.480
7.459
6.904
6.883
6.321
6.281
4.901
4.890
4.879
4.870
4.857
4.848
3.828
1.916
1.903
1.781
1.771
1.757
1.584
1.573
1.554
1.533
1.502
1.476
1.448
1.419
1.387
1.361
1.325
1.300
1.270
1.01
2.02
2.00
1.00
1.00
3.05
2.12
2.14
6.55
8.0 7.5 7.0 6.5 6.0 5.5 5.0 4.5 4.0 3.5 3.0 2.5 2.0 1.5 1.0 0.5 0.0 ppm
166.52
161.04
143.66
129.40
127.10
116.20
114.06
77.13
76.81
76.49
72.28
55.12
31.57
25.25
23.62
170 160 150 140 130 120 110 100 90 80 70 60 50 40 30 20 10 0 ppm

8b:

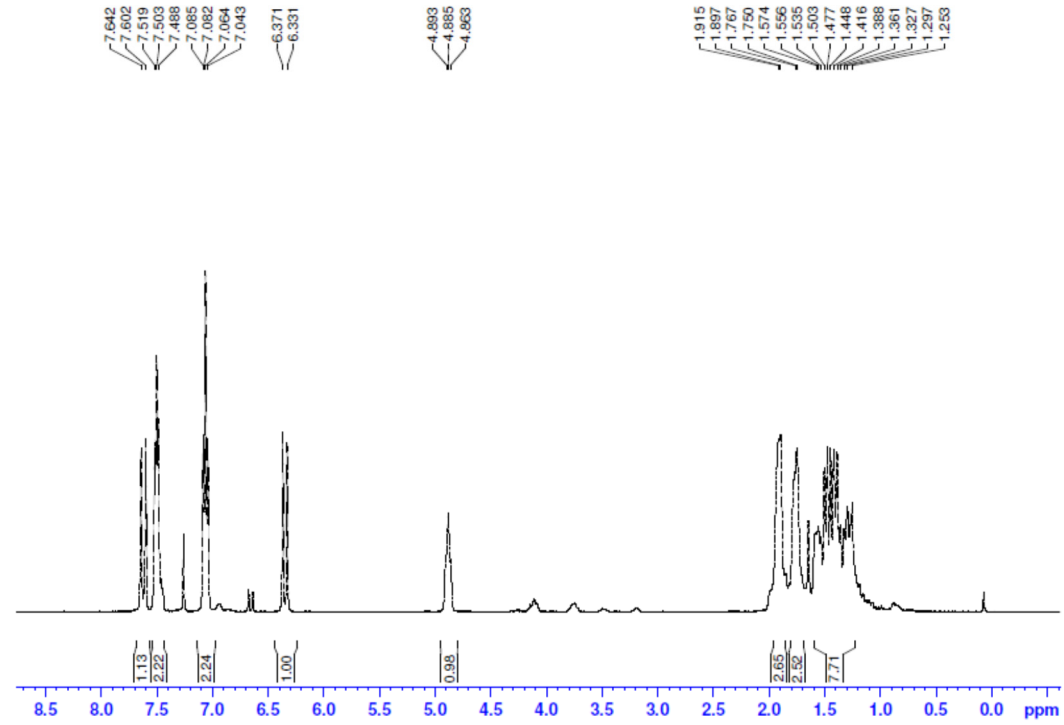
7.642
7.602
7.519
7.503
7.488
7.085
7.082
7.064
7.043
6.371
6.331
4.893
4.885
4.863
1.915
1.897
1.767
1.750
1.574
1.556
1.535
1.503
1.477
1.448
1.416
1.388
1.361
1.327
1.297
1.253
1.13
2.22
2.24
1.00
0.98
2.65
2.62
7.71
8.5 8.0 7.5 7.0 6.5 6.0 5.5 5.0 4.5 4.0 3.5 3.0 2.5 2.0 1.5 1.0 0.5 0.0 ppm

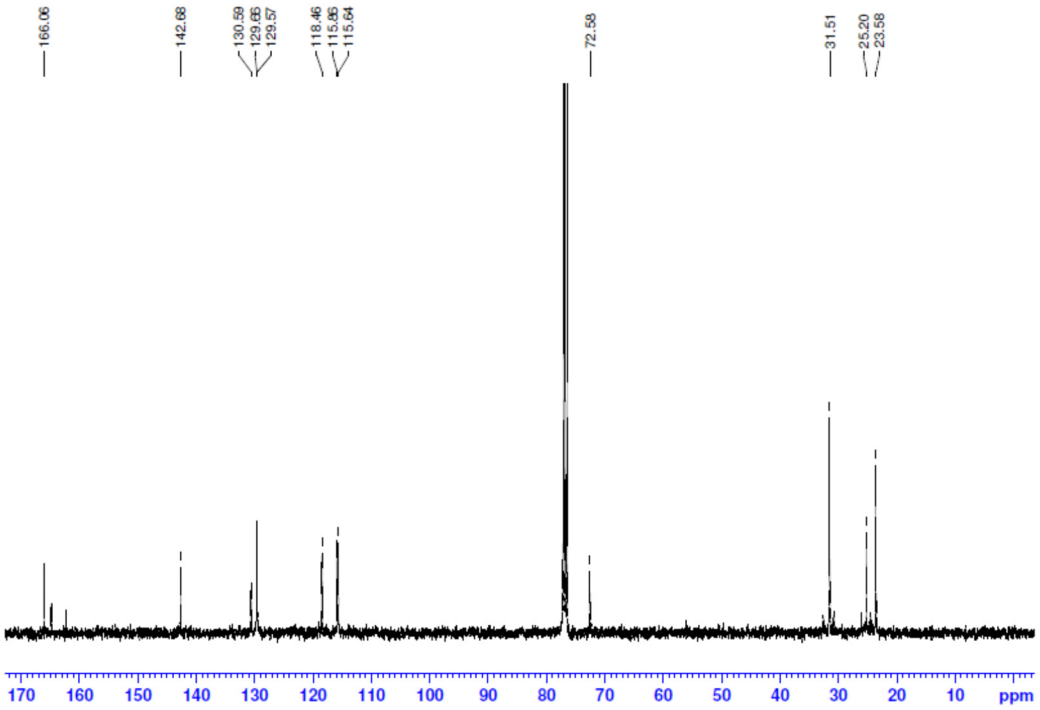
166.06
142.68
130.59
129.65
129.57
118.46
115.85
115.64
72.58
31.51
25.20
23.58
170 160 150 140 130 120 110 100 90 80 70 60 50 40 30 20 10 ppm

9b:

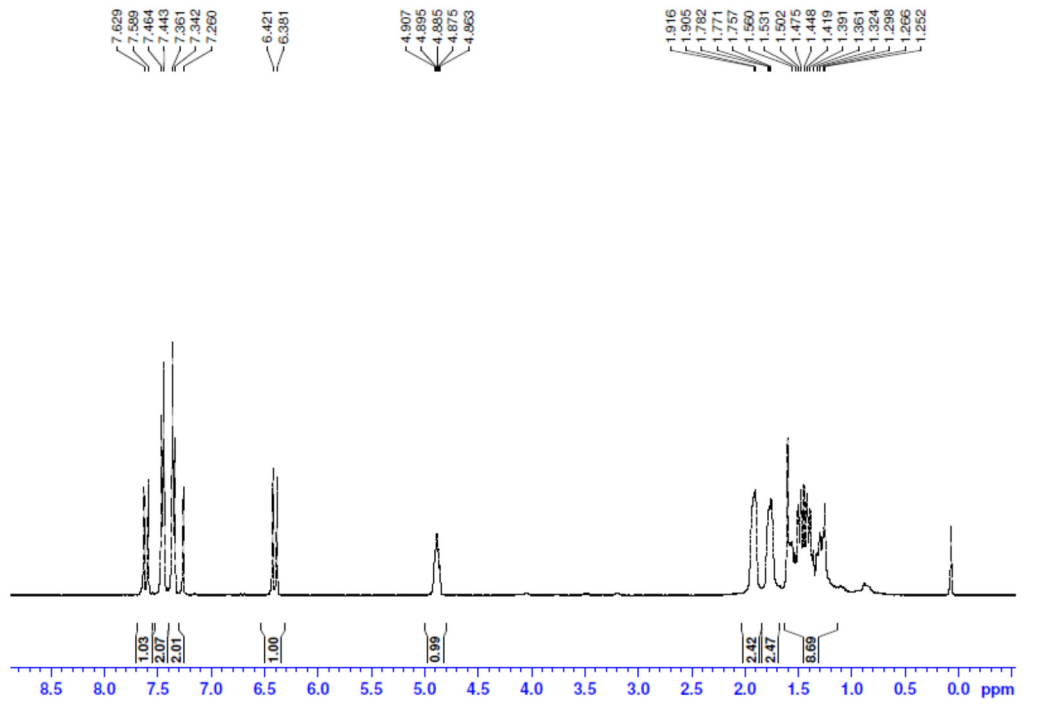
7.629
7.589
7.464
7.443
7.361
7.342
7.260
6.421
6.381
4.907
4.895
4.885
4.875
4.863
1.916
1.905
1.782
1.771
1.757
1.560
1.531
1.502
1.475
1.448
1.419
1.391
1.361
1.324
1.298
1.266
1.252
1.09
2.07
2.01
1.00
0.99
2.42
2.47
8.69
8.5 8.0 7.5 7.0 6.5 6.0 5.5 5.0 4.5 4.0 3.5 3.0 2.5 2.0 1.5 1.0 0.5 0.0 ppm

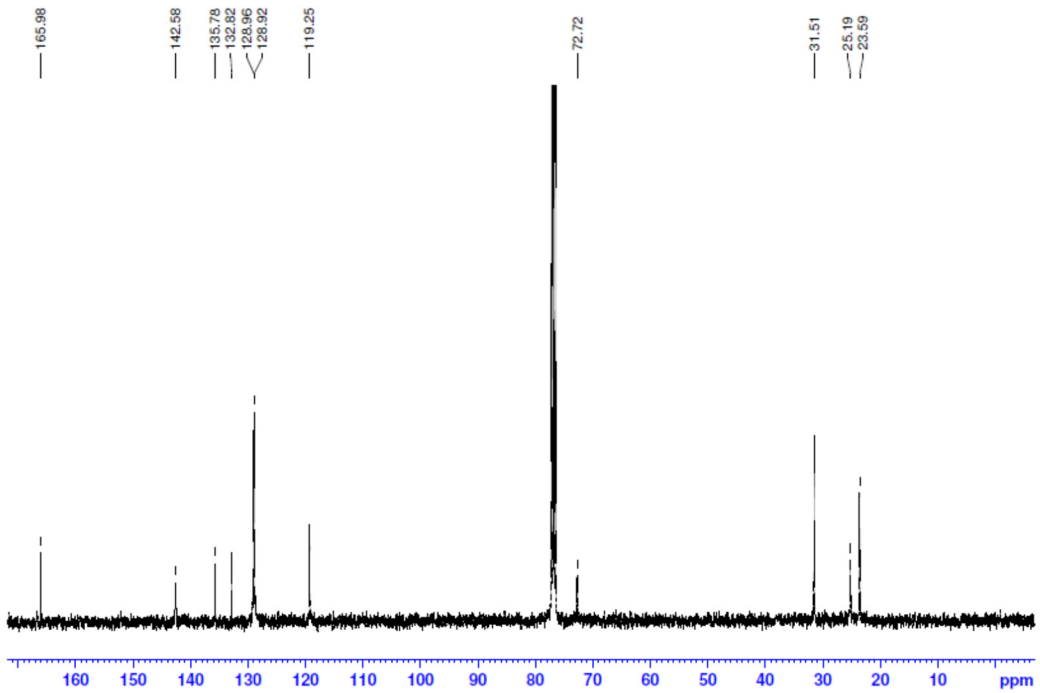
165.98
142.58
135.78
132.82
128.96
128.92
119.25
72.72
31.51
25.19
23.59
160 150 140 130 120 110 100 90 80 70 60 50 40 30 20 10 ppm

10b:

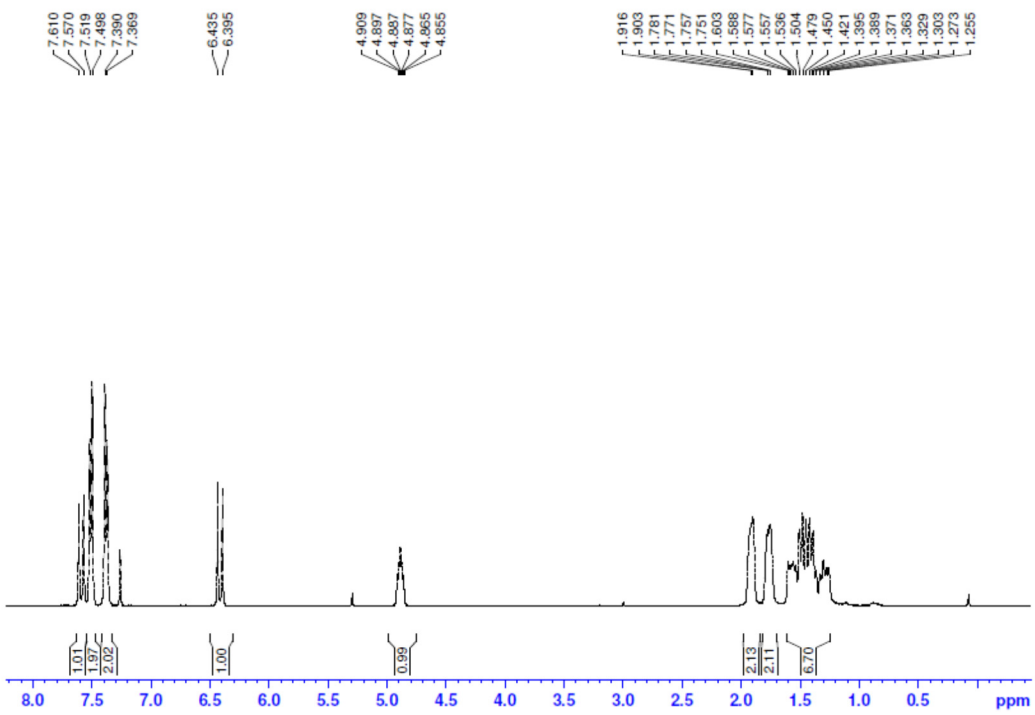
7.610
7.570
7.519
7.498
7.390
7.369
6.435
6.395
4.909
4.897
4.887
4.877
4.865
4.855
1.916
1.903
1.781
1.771
1.757
1.751
1.603
1.588
1.577
1.557
1.536
1.504
1.479
1.450
1.421
1.395
1.389
1.371
1.363
1.329
1.303
1.273
1.255
1.01
1.97
2.02
1.00
0.99
2.13
2.11
6.70
8.0
7.5
7.0
6.5
6.0
5.5
5.0
4.5
4.0
3.5
3.0
2.5
2.0
1.5
1.0
0.5
ppm

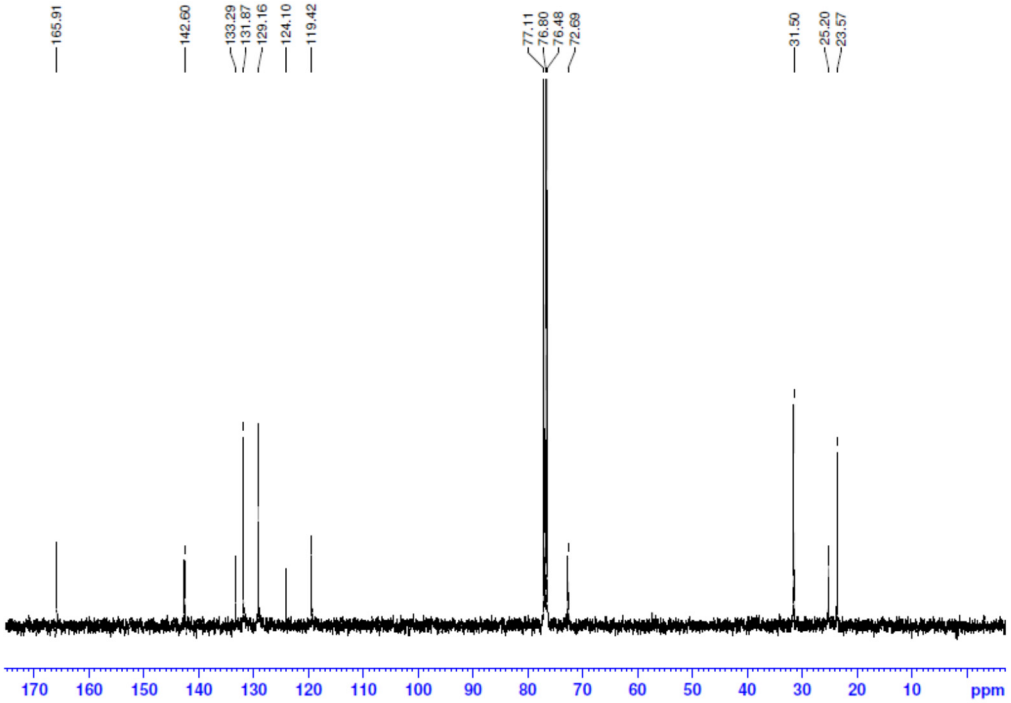
165.91
142.60
133.29
131.87
129.16
124.10
119.42
77.11
76.80
76.48
72.69
31.50
25.20
23.57
170
160
150
140
130
120
110
100
90
80
70
60
50
40
30
20
10
ppm

11b:

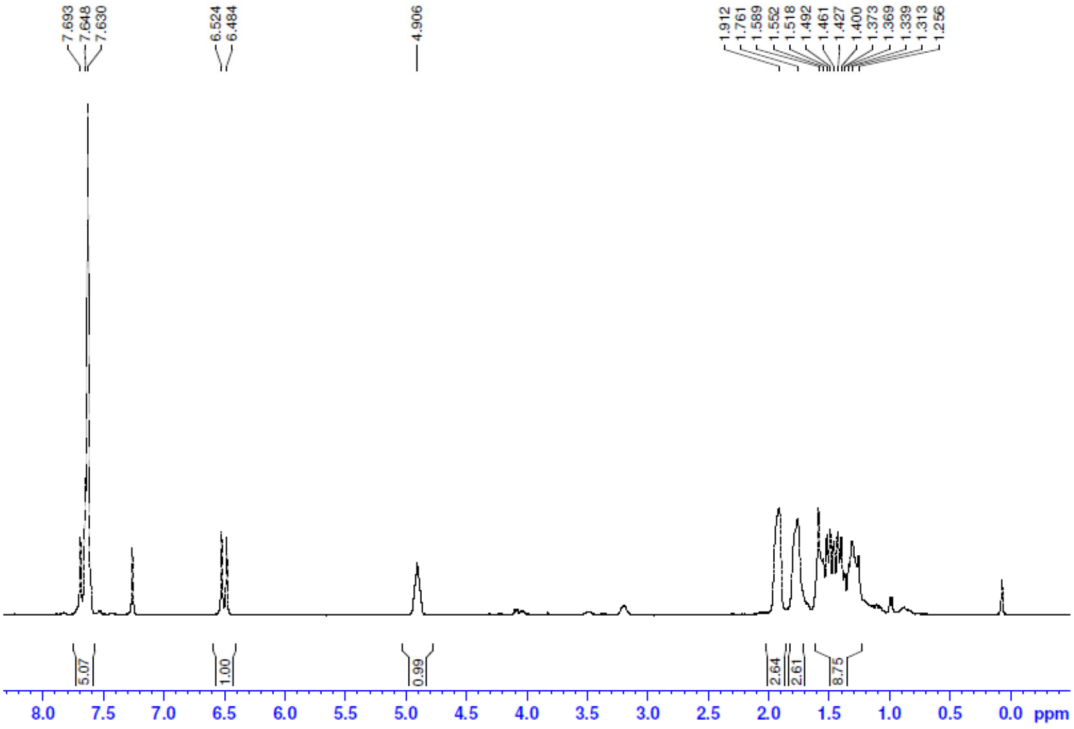
7.693
7.648
7.630
6.524
6.484
4.906
1.912
1.761
1.589
1.552
1.518
1.492
1.461
1.427
1.400
1.373
1.369
1.339
1.313
1.256
5.07
1.00
0.99
2.64
2.61
8.75
8.0 7.5 7.0 6.5 6.0 5.5 5.0 4.5 4.0 3.5 3.0 2.5 2.0 1.5 1.0 0.5 0.0 ppm

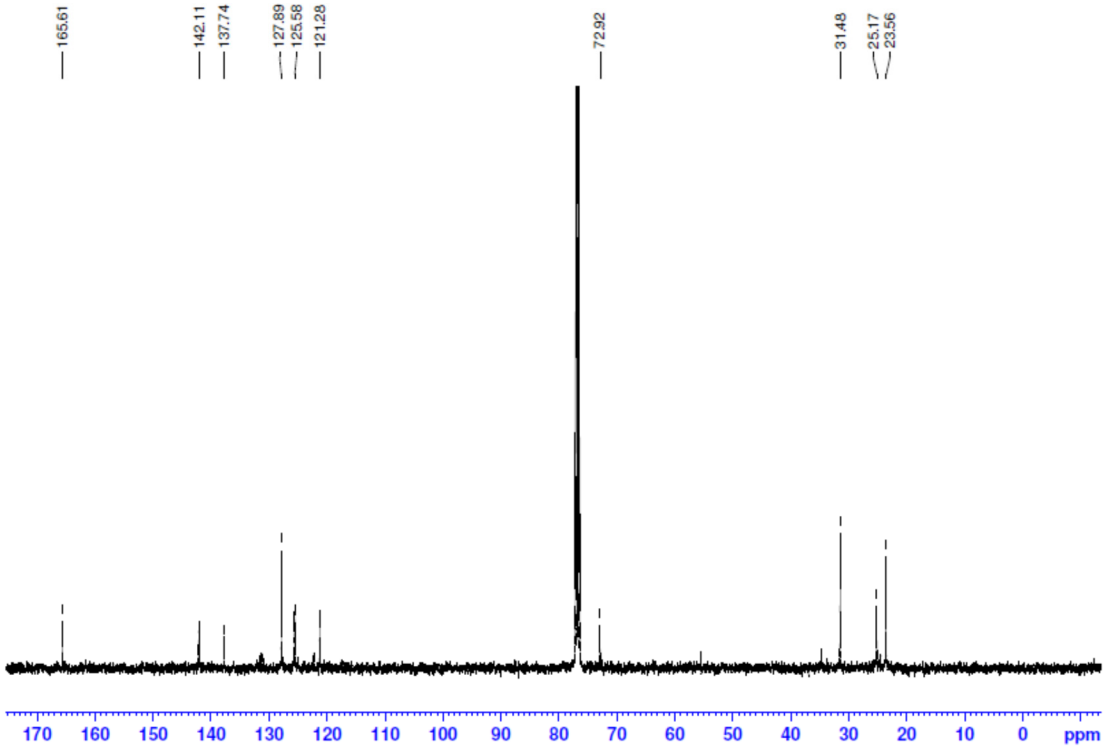
165.61
142.11
137.74
127.89
125.58
121.28
72.92
31.48
25.17
23.56
170 160 150 140 130 120 110 100 90 80 70 60 50 40 30 20 10 0 ppm

12b:

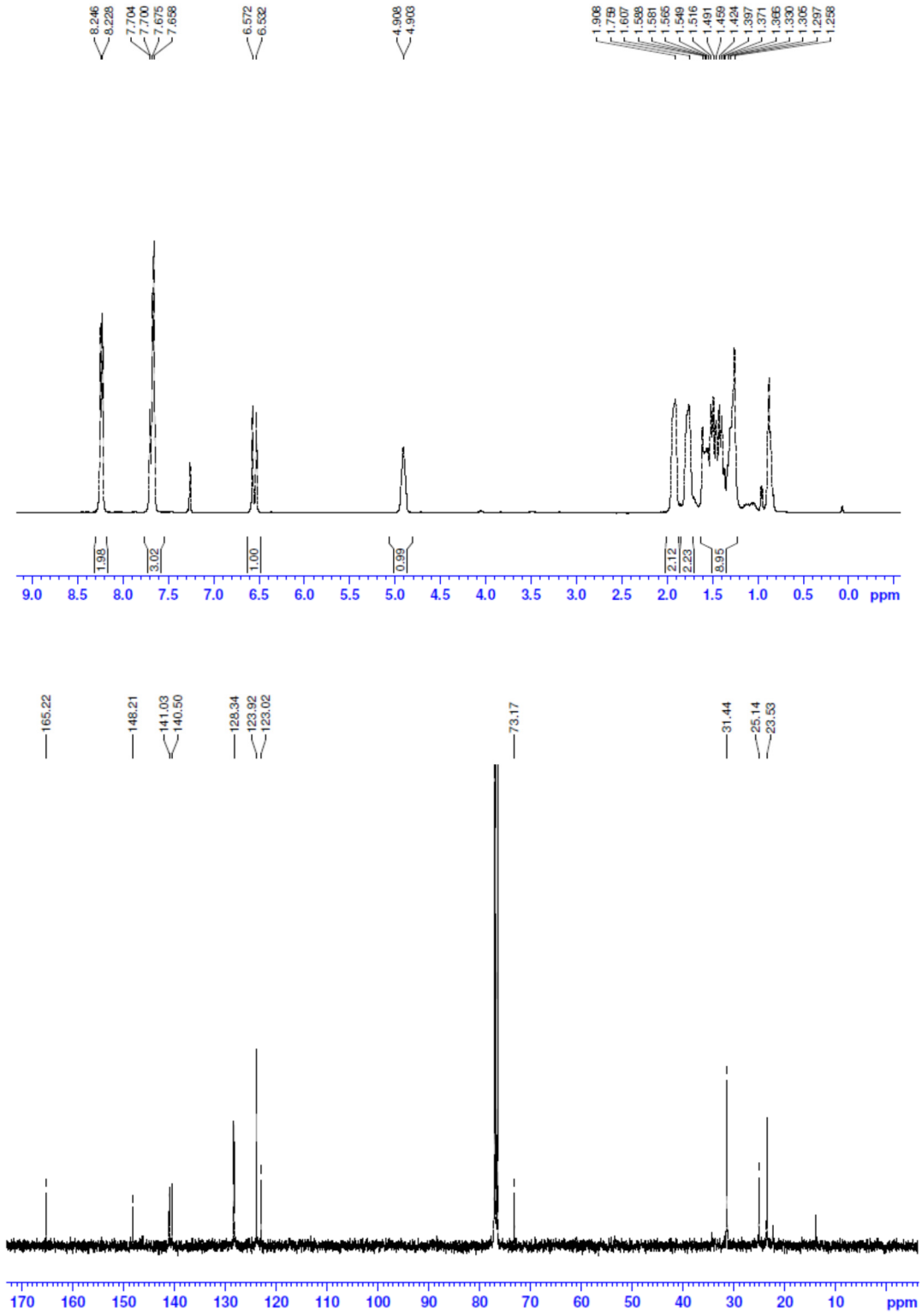
8.246
8.228
7.704
7.700
7.675
7.658
6.572
6.532
4.908
4.903
1.908
1.759
1.607
1.598
1.581
1.565
1.549
1.516
1.491
1.459
1.424
1.397
1.371
1.330
1.305
1.297
1.258
1.98
3.02
1.00
0.99
2.12
2.23
8.95
9.0 8.5 8.0 7.5 7.0 6.5 6.0 5.5 5.0 4.5 4.0 3.5 3.0 2.5 2.0 1.5 1.0 0.5 0.0 ppm
165.22
148.21
141.03
140.50
128.34
123.92
123.02
73.17
31.44
25.14
23.53
170 160 150 140 130 120 110 100 90 80 70 60 50 40 30 20 10 ppm

13b:

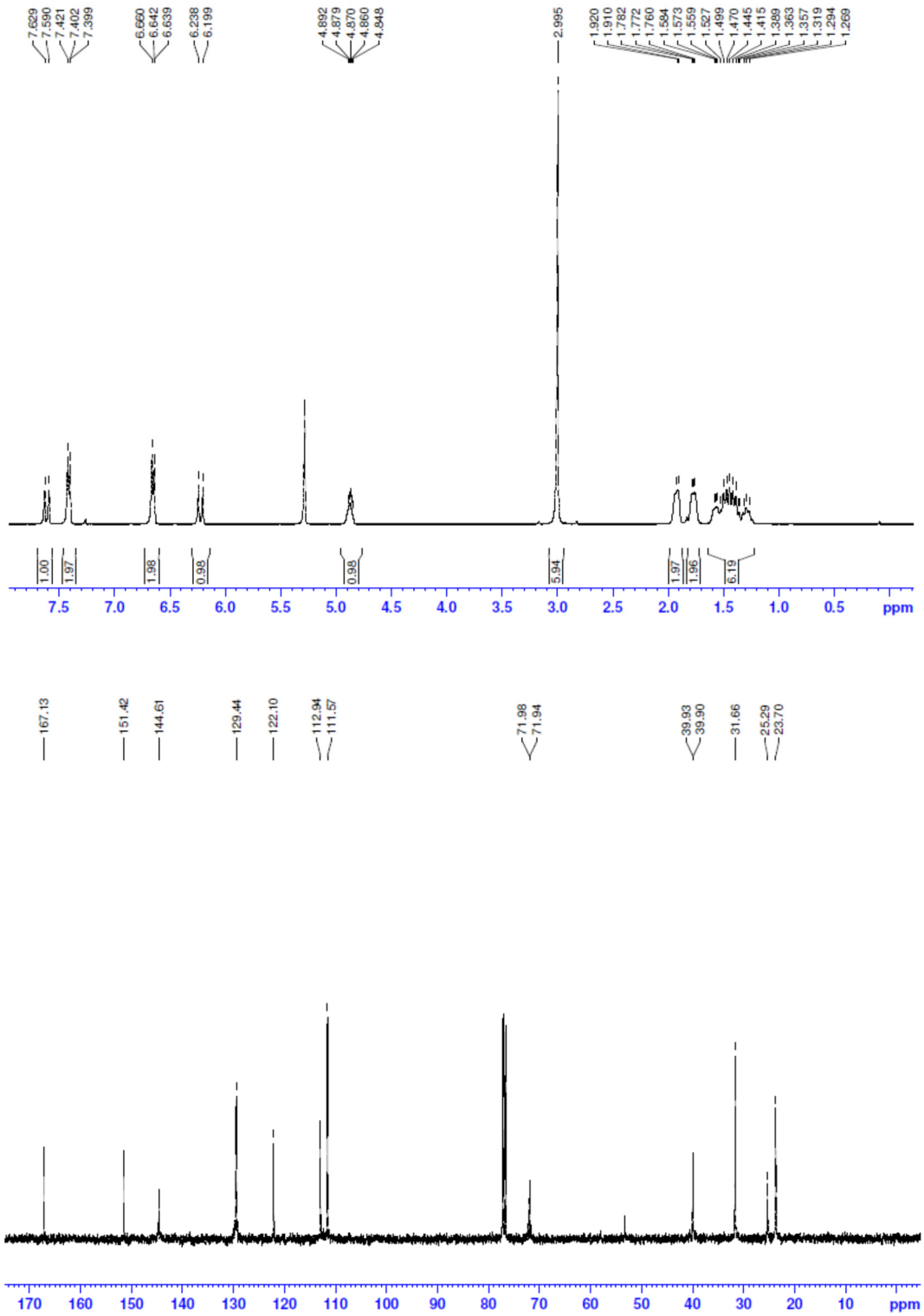
7.629
7.590
7.421
7.402
7.399
6.660
6.642
6.639
6.238
6.199
4.892
4.879
4.870
4.860
4.848
2.995
1.920
1.910
1.782
1.772
1.760
1.584
1.573
1.559
1.527
1.499
1.470
1.445
1.415
1.389
1.363
1.357
1.319
1.294
1.269
1.00
1.97
1.98
0.98
0.98
5.94
1.97
1.96
6.19
7.5 7.0 6.5 6.0 5.5 5.0 4.5 4.0 3.5 3.0 2.5 2.0 1.5 1.0 0.5 ppm
167.13
151.42
144.61
129.44
122.10
112.94
111.57
71.98
71.94
39.93
39.90
31.66
25.29
23.70
170 160 150 140 130 120 110 100 90 80 70 60 50 40 30 20 10 ppm

14b:

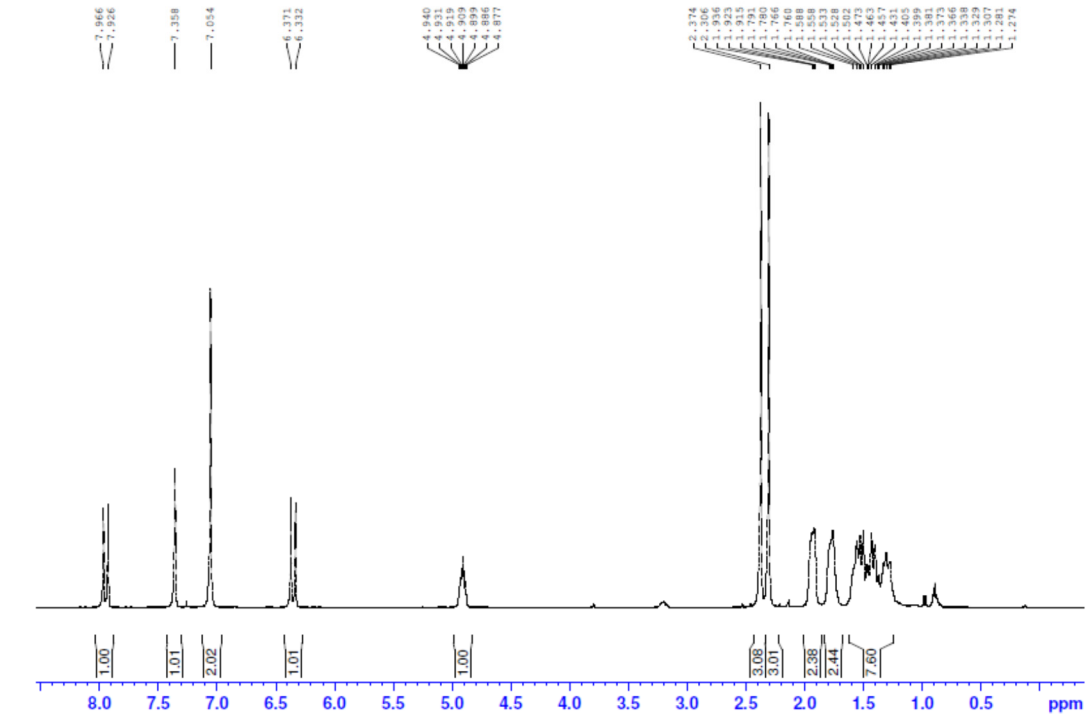
7.966
7.926
7.358
7.054
6.371
6.332
4.940
4.921
4.919
4.909
4.899
4.886
4.877
2.374
2.356
2.336
1.923
1.915
1.791
1.780
1.766
1.746
1.588
1.558
1.533
1.528
1.502
1.473
1.463
1.457
1.431
1.405
1.399
1.393
1.373
1.366
1.338
1.329
1.307
1.281
1.274
1.00
1.01
2.02
1.01
1.00
3.08
3.01
2.38
2.44
7.60
8.0
7.5
7.0
6.5
6.0
5.5
5.0
4.5
4.0
3.5
3.0
2.5
2.0
1.5
1.0
0.5
ppm

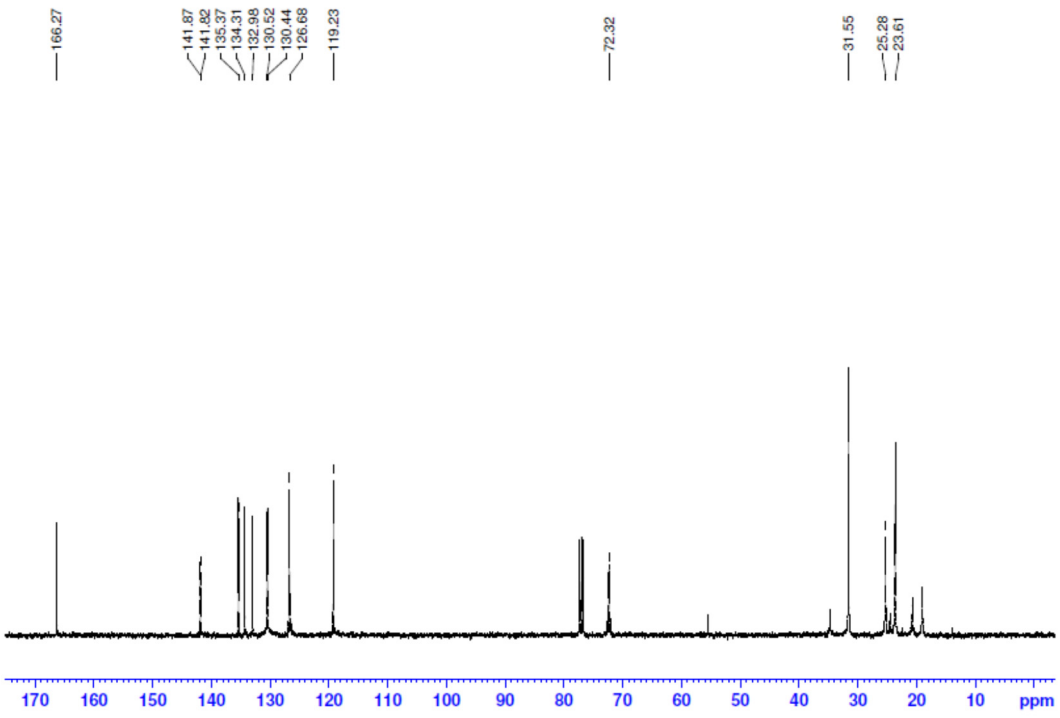
166.27
141.87
141.82
135.37
134.31
132.98
130.52
130.44
126.68
119.23
72.32
31.55
25.28
23.61
170
160
150
140
130
120
110
100
90
80
70
60
50
40
30
20
10
ppm

15b:

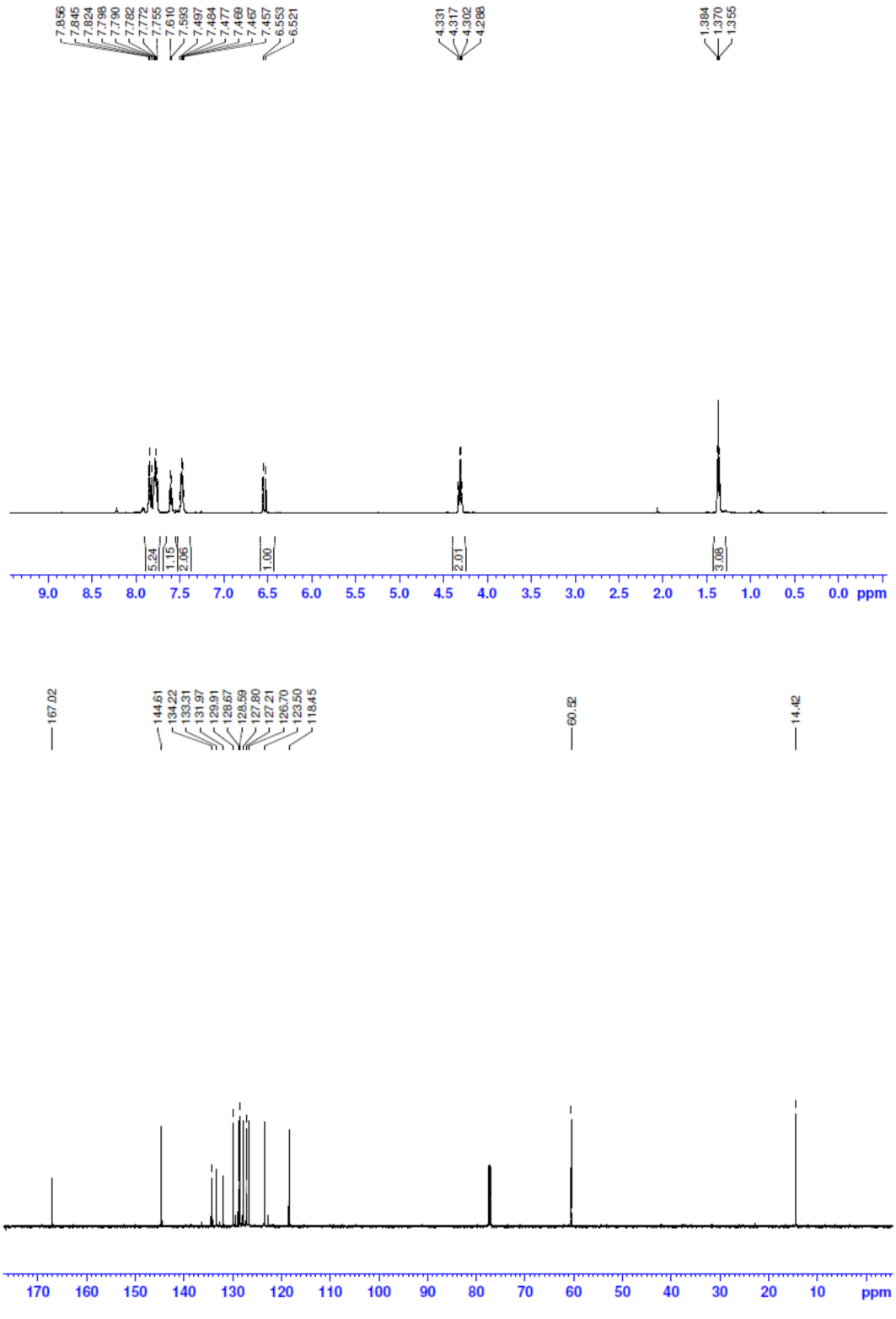
7.856
7.845
7.824
7.798
7.790
7.782
7.772
7.755
7.610
7.593
7.497
7.484
7.477
7.469
7.467
7.457
6.553
6.521
4.331
4.317
4.302
4.288
1.384
1.370
1.355
5.24
1.15
2.06
1.00
2.01
3.08
9.0 8.5 8.0 7.5 7.0 6.5 6.0 5.5 5.0 4.5 4.0 3.5 3.0 2.5 2.0 1.5 1.0 0.5 0.0 ppm
167.02
144.61
134.22
133.31
131.97
129.91
128.67
128.59
127.80
127.21
126.70
123.50
118.45
60.52
14.42
170 160 150 140 130 120 110 100 90 80 70 60 50 40 30 20 10 ppm

16b:

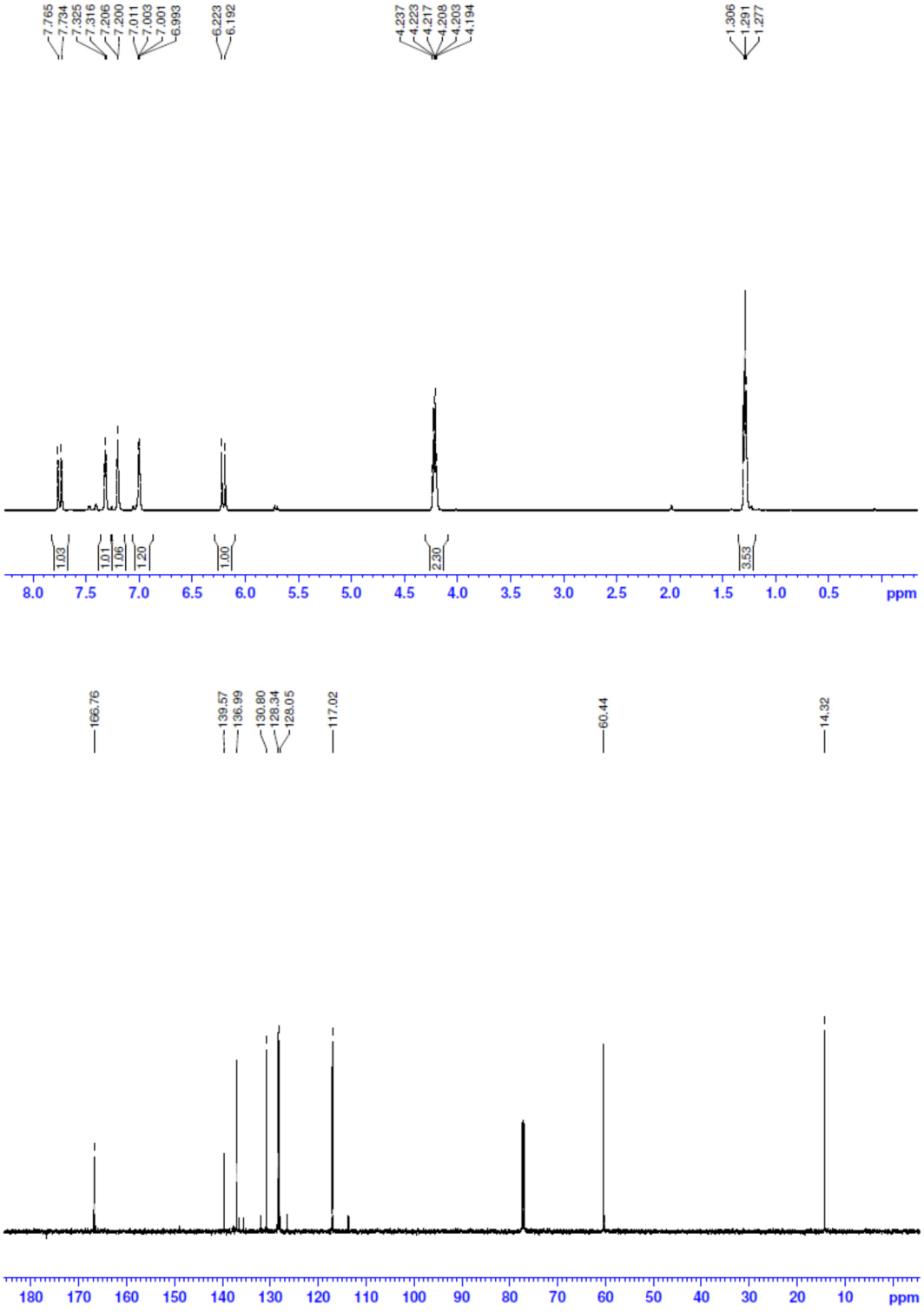
7.765
7.734
7.325
7.316
7.206
7.200
7.011
7.003
7.001
6.993
6.223
6.192
4.237
4.223
4.217
4.208
4.203
4.194
1.306
1.291
1.277
1.03
1.01
1.06
1.20
1.00
2.30
3.53
8.0 7.5 7.0 6.5 6.0 5.5 5.0 4.5 4.0 3.5 3.0 2.5 2.0 1.5 1.0 0.5 ppm
166.76
139.57
136.99
130.80
128.34
128.05
117.02
60.44
14.32
180 170 160 150 140 130 120 110 100 90 80 70 60 50 40 30 20 10 ppm

17b:

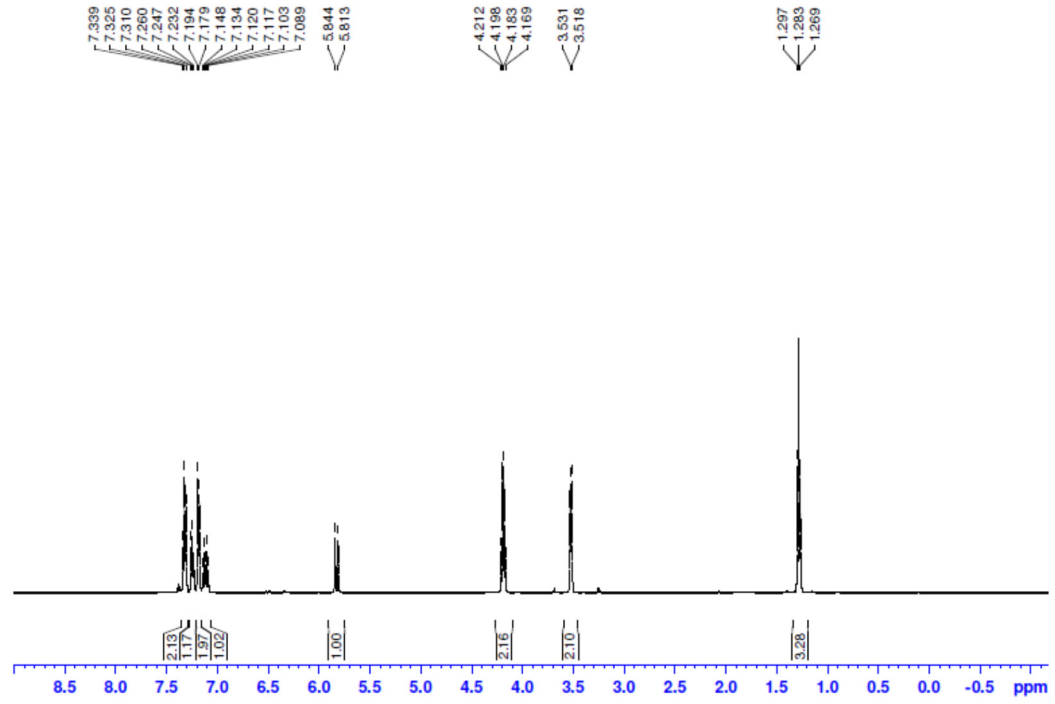
7.339
7.325
7.310
7.260
7.247
7.232
7.194
7.179
7.148
7.134
7.120
7.117
7.103
7.089
5.844
5.813
4.212
4.198
4.183
4.169
3.531
3.518
1.297
1.283
1.269
2.13
1.17
1.97
1.02
1.00
2.16
2.10
3.28
8.5 8.0 7.5 7.0 6.5 6.0 5.5 5.0 4.5 4.0 3.5 3.0 2.5 2.0 1.5 1.0 0.5 0.0 -0.5 ppm

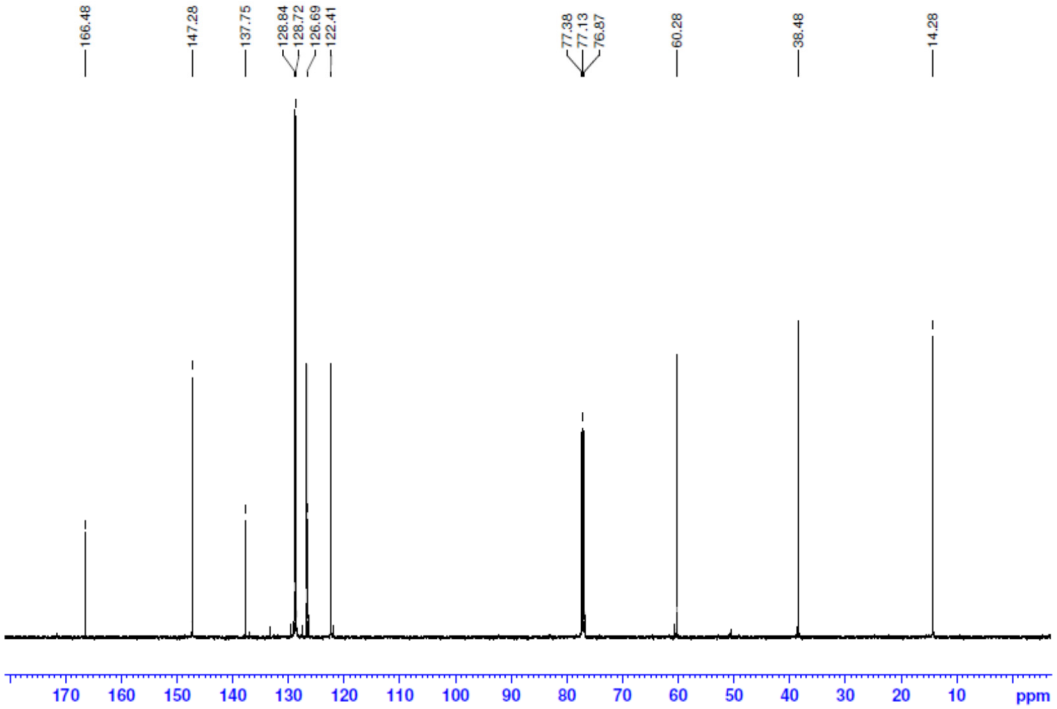
166.48
147.28
137.75
128.84
128.72
126.69
122.41
77.38
77.13
76.87
60.28
38.48
14.28
170 160 150 140 130 120 110 100 90 80 70 60 50 40 30 20 10 ppm